Electrostatic Noise Bands Associated with the Electron Gyrofrequency and Plasma Frequency in the Outer Magnetosphere

by

Robert Russell Shaw

A thesis submitted in partial fulfillment of the requirements for the degree of Doctor of Philosophy in the Department of Physics and Astronomy in the Graduate College of The University of Iowa

July, 1975

Thesis supervisor: Professor Donald A. Gurnett

Graduate College
The University of Iowa
Iowa City, Iowa

CERTIFICATE OF APPROVAL

PH.D. THESIS

This is to certify that the Ph.D. thesis of

Robert Russell Shaw

has been approved by the Examining Committee for the thesis requirement for the Doctor of Philosophy degree in the Department of Physics and Astronomy at the July, 1975 graduation.

Thesis committee:

Thesis supervisor

Member

Member

Member

Member

ACKNOWLEDGMENTS

I thank Dr. Norman Ness and Dr. Donald Fairfield for providing measurements of the geomagnetic field strength made by the NASA/GSFC magnetometer experiment on board IMP 6. Dr. James Van Allen provided encouragement and support while I was a student at the University of Iowa. I am indebted to my advisor, Dr. Donald A. Gurnett, as principal investigator of the University of Iowa IMP 6 plasma wave experiment. His encouragement, advice, support, and instruction have been invaluable to me both professionally and personally.

I thank Dora Walker and our staff of undergraduate research aides who skillfully process our wideband data. I owe a special thanks to Richard West, who aided with much of the data reduction, and to William Kurth and Geary Voots who developed computer programs used to analyze the digital data and also assisted in the data analysis. John Birkbeck and Joyce Chrisinger expertly drafted the figures, and Sandy Van Engelenhoven rapidly and accurately typed the manuscript. I appreciate the industry and encouragement of my wife, Barbara, who helped support our family during my years in graduate school.

This research was supported in part by the National Aeronautics and Space Administration under Contract NAS5-11704 and Grant NGL-16-001-043 and by the Office of Naval Research under Grant N00014-68-A-0196-0009.

TABLE OF CONTENTS

LIST OF FIGURES

Page

Page

ABSTRACT

Naturally occurring noise bands near the electron plasma frequency are frequently detected by the University of Iowa plasma wave experiment on the IMP 6 satellite in the region from just inside the plasmapause to radial distances of about 10 earth radii in the outer magnetosphere. The electric field strength of these noise bands is usually small with electric field spectral densities typically near 10^{-15} volts^2 meter^{-2} Hz^{-1} (broadband field strengths of about two microvolts per meter). A wave magnetic field has been detected only in a few unusually intense cases, and in these cases the magnetic field energy density is several orders of magnitude smaller than the electric field energy density. The bands are observed at all magnetic latitudes covered by the IMP 6 orbit ($|\lambda_m| \leq 45°$) and appear to be a permanent feature of the outer magnetosphere. They are found at all local times and occur least frequently in the quadrant from 18 to 24 hours. The bands appear to consist of two distinct spectral types which we have called diffuse and narrow band. In both types the center frequency of the noise band is bounded by consecutive harmonics of the electron gyrofrequency, and the bands occur most often between harmonics that are near the local electron plasma frequency. These bands appear to merge continuously into two types of plasma wave emissions that are found in dissimilar regions of the magnetosphere

(upper hybrid resonance noise, also called Region 3 noise, inside the plasmasphere and $(n + 1/2)f_g$ harmonics in the outer magnetosphere). It is suggested that this smooth merging is caused by changes in the plasma wave dispersion relation that occur as the spacecraft moves from the cold plasma within the plasmasphere into the warm, non-Maxwellian plasma found in the outer magnetosphere.

I. INTRODUCTION

The earth's magnetosphere has provided an excellent natural laboratory for studying the generation of various types of plasma waves. The large physical size of spatial inhomogenieties and the large wavelengths of many types of waves enables one to neglect boundary effects that can complicate the interpretation of data gathered in ground laboratory experiments.

The electric and magnetic fields of naturally occurring plasma waves can interact with the charged particles that populate different regions of the magnetosphere. Wave-particle interactions can result in the generation and absorption of wave energy and changes in the constituent particle energy distributions. Thus, these types of interactions may explain some of the dynamics of the magnetosphere.

Electrostatic waves are particularly interesting because these waves often have phase velocities that are comparable to the thermal speeds of the constituent particles of the plasma. Thus, electrostatic instabilities usually play an important role in studying fluctuations and instabilities in laboratory plasmas. Electrostatic modes that interact primarily with thermal electrons should occur at frequencies near the electron plasma frequency, f_p, the electron gyrofrequency, f_g, and the upper hybrid resonance frequency, f_{UHR}.

These frequencies are natural resonant frequencies at which instabilities generated by the thermal motions of the electrons can most easily occur.

A variety of plasma wave emissions have been observed by rocket- and satellite-borne radio noise experiments at frequencies near these three resonant frequencies. A noise band that is found at frequencies between the local plasma frequency and the local upper hybrid resonance frequency has been observed in the ionosphere and plasmasphere by Walsh et al. [1964]; Bauer and Stone [1968]; Gregory [1969]; Muldrew [1970]; and Hartz [1970]. More recently, Mosier et al. [1973] reported observations of a similar noise band (which we call upper hybrid resonance noise) inside the plasmasphere at frequencies between the local plasma and upper hybrid resonance frequencies. This type of noise has also been called Region 3 noise because it occurs in Region 3 of the CMA diagram that describes wave propagation in a cold plasma [see Stix, 1962]. Incoherent Cerenkov radiation from thermal electrons is believed to generate upper hybrid resonance noise, and the propagation of the wave energy appears to be adequately described by cold plasma theory [see Mosier et al., 1973; Taylor and Shawhan, 1974].

Intense narrow band electrostatic emissions (called $(n + 1/2)f_g$ harmonics) have been detected in the outer magnetosphere by OGO 5 with wave frequencies between harmonics of the local electron gyrofrequency [Kennel et al., 1970; Fredricks and Scarf, 1973; Scarf et al., 1973]. The generation of the $(n + 1/2)f_g$ harmonics cannot be understood

in terms of cold plasma theory. Instead, an electrostatic instability driven by a non-Maxwellian electron velocity distribution is believed to generate these waves [see Fredricks, 1971; Young et al., 1973].

Weak electromagnetic continuum radiation (called $f > f_p$ noise) has been observed trapped in the outer magnetosphere at frequencies just above the local electron plasma frequency [Gurnett and Shaw, 1973]. In some cases this radiation has a sharp lower cutoff at the local electron plasma frequency that provides an accurate determination of the electron number density [Gurnett and Frank, 1974].

The University of Iowa plasma wave experiment on board the IMP 6 satellite has detected electrostatic noise bands in the outer magnetosphere that occur between harmonics of the local electron gyrofrequency at frequencies near the local plasma frequency. These emissions are found throughout a large region of the magnetosphere, occurring from well inside the plasmapause to radial distances as great as ten earth radii. Such bands are detectable on about two-thirds of all the IMP 6 magnetospheric passes and are essentially a permanent feature of the magnetosphere. These bands typically have small electric field amplitudes, with broad-band field strengths usually about two microvolts per meter, and they probably have not been previously observed because of the low amplitudes at which they occur.

The characteristics of these electrostatic noise bands change as the spacecraft moves from inside the plasmasphere to larger radial distances in the outer magnetosphere. Well inside the plasmasphere

the noise bands have characteristics similar to upper hybrid resonance noise, while at larger radial distances in the outer magnetosphere the noise bands often develop characteristics similar to the $(n + 1/2)f_g$ harmonics. Thus, these observations suggest that there is a continuous transition connecting these two different types of naturally occurring noise that are found in dissimilar regions of the magnetosphere.

This paper describes the University of Iowa IMP 6 plasma wave experiment, presents an observational study of the diffuse and narrow-band electrostatic noise observed by the University of Iowa experiment, and suggests an explanation for the smooth transition between these noise bands and the other types of noise found in the plasmasphere and the outer magnetosphere.

II. DESCRIPTION OF THE EXPERIMENT

A. IMP 6 Orbit

IMP 6 is one of a series of spacecraft that were designed for the purpose of studying the earth's magnetosphere, the bow shock, the geomagnetic tail, and the solar wind. IMP 6 carried twelve scientific experiments, one of which is a plasma wave experiment designed and built at the University of Iowa. The data surveyed for this report were collected during the first year of operation of the experiment, which measures plasma wave phenomena in the frequency range 20 Hz to 200 kHz.

The IMP 6 spacecraft was launched on March 13, 1971, from the Eastern Test Range at Cape Kennedy, Florida. The highly elliptical orbit had an initial perigee and apogee at geocentric radial distances of 6610 km and 212,630 km, respectively. The radial distance of perigee increased to a maximum of about 20,000 km in December, 1972, and then it decreased progressively until burn-up in the atmosphere in October, 1974. The orbit inclination was 28.7 degrees, and the period was slightly greater than 100 hours. The spacecraft was spin-stabilized, rotating with a period of about eleven seconds about the z-axis which was oriented normal to the ecliptic plane.

Figure 1 is a projection of an IMP 6 orbit on the ecliptic plane. The position of the spacecraft is described in spherical

coordinates defined by the geocentric radial distance, the angle from the antisunward direction to the projection of the radius vector in the ecliptic plane (local time), and the angle from the radius vector to the ecliptic plane (solar ecliptic latitude). The major axis of the orbit rotates through twenty-four hours of local time per year so that a nearly uniform sampling of all local times is achieved in one year.

Figure 1 shows the regions in the magnetosphere that are sampled by the IMP 6 orbit. At low altitudes the spacecraft is located within the plasmasphere, which consists of a region containing cold plasma co-rotating with the earth. This plasma is believed to have its source in the ionosphere, and its temperature is probably of the order of a few electron volts. The electron number density ranges from 10^4 cm^{-3} near the ionosphere to 10^3 cm^{-3} near the inside edge of the plasmapause boundary.

At geocentric radial distances near five earth radii in the equatorial plane the plasmapause is found. At the plasmapause the number density of the plasma abruptly drops by two to three orders of magnitude. Ion number densities are typically measured at 1 cm^{-3} to 10 cm^{-3} just outside the plasmapause. In addition, the earthward edge of the plasma sheet is found near the outside edge of the plasmasphere.

The plasma sheet is a region containing a warm, low density plasma that extends to large radial distances in the geomagnetic tail. Typical plasma sheet electron number densities are of the order of

1 cm^{-3}, and average electron energies are of the order of 100 eV to a few keV. The plasma sheet extends to large distances in the geomagnetic tail ($> 60\ R_E$) averaging about seven earth radii thick and about 40 earth radii wide. In the equatorial plane the plasma sheet fills most of the region between the plasmapause and the magnetopause boundary shown in Figure 1.

As the IMP 6 spacecraft moves from inside the plasmasphere, through the plasmapause into the plasma sheet, and through the magnetopause, the characteristics of the plasma surrounding the spacecraft change significantly. Inside the plasmasphere the plasma is a cold, high density plasma. The propagation characteristics of most wave modes are described by the theory of wave propagation in a cold magnetoplasma [see Stix, 1962].

Inside the plasma sheet, however, the thermal energy of the electrons is several orders of magnitude greater and the number density is several orders of magnitude less than those observed inside the plasmasphere. Thus, thermal effects may be more important for explaining the generation and propagation of plasma waves than the interactions between the plasma and the geomagnetic field.

The spacecraft moves from perigee inside the plasmasphere to the dayside magnetopause boundary in about five hours, so that the spacecraft is at radial distances below ten earth radii in the magnetosphere approximately ten percent of the time. Thus, although the spacecraft is outside the magnetosphere the majority of the time, a sampling of the magnetosphere below ten earth radii can be obtained

in a relatively short time. This characteristic of the orbit makes it possible to continuously examine changes in the generation and propagation of naturally occurring emissions in different regions of the magnetosphere under relatively unchanging magnetospheric conditions.

B. University of Iowa Plasma Wave Experiment

The University of Iowa plasma wave experiment consists of a complement of electric dipole and magnetic loop antennas, two identical frequency spectrum analyzers, and two broadband AGC receivers. Seven different antennas are used by the experiment to detect both electrostatic and electromagnetic plasma wave phenomena.

Figure 2 is a drawing of the IMP 6 spacecraft showing these antennas in the deployed configuration. The three electric "long-wire" dipole antennas are composed of twin cylindrical copper elements that are extended from the main body of the spacecraft in flight. The E_x and E_y antennas, which are perpendicular to the spin axis of the spacecraft, have tip-to-tip lengths of 54.0 meters and 93.2 meters, respectively. The third long antenna, E_z, is parallel to the spin axis and has a tip-to-tip length of 6.55 meters. The fourth antenna is a "short electric" dipole antenna that is mounted on the magnetometer boom. This antenna consists of two wire cage spherical elements with a center-to-center separation of 0.38 meters in the z direction. The short electric antenna is used for the detection of waves with wavelengths that are short compared to the dimensions of the long electric antennas.

The magnetic loop antennas consist of three mutually orthogonal one turn loops, each with an area of slightly less than one square meter. The loop antenna assembly is mounted on a boom that extends approximately four meters from the body of the spacecraft, and each antenna is coupled to a preamplifier through a transformer with a turns ratio of 250:1.

Several combinations of these antennas may be connected to either of two identical spectrum analyzers as shown in Figure 3. Each spectrum analyzer consists of sixteen filter channels with bandwidths of about fifteen percent of the center frequency. There are four filter channels for each decade in frequency, covering the frequency range from 20 Hz to 200 kHz. The signal from each filter channel is applied to a logarithmic compressor which consists of five successive amplifier stages, each of which saturates for signals which differ in amplitude by about one order of magnitude. These outputs are then added by a summing amplifier and converted to a d.c. voltage by one of two detectors, a peak detector or an average detector. Thus, the output of each detector is a d.c. voltage that is approximately proportional to the logarithm of the signal amplitude at the input of the compressor.

The peak detector measures the largest signal strength seen during each sample interval of 5.11 seconds. It has a time constant equal to 0.1 seconds, and it is reset to zero at the start of each new sample interval. The average detector has a time constant equal to the sample interval; therefore, it continuously measures a signal strength that is time averaged over a 5.11 second interval.

Each filter channel has a dynamic range of 100 db with a sensitivity of less than 10 microvolts for a sine wave signal at the center frequency of the filter channel. Operated in conjunction with the long electric antennas, electric field strengths as low as 0.2 microvolts per meter can be measured. The sensitivity of the magnetic loop antennas is a function of frequency and varies from about 2.0 milligammas at 36 Hz to about 10.0 microgammas at 16.5 kHz.

In addition to the peak and average detectors described above, each spectrum analyzer has four rapid sample detectors at 35 Hz, 311 Hz, 3.11 kHz, and 31.1 kHz, each of which has a time constant of 0.1 seconds and a sample interval of 0.32 seconds. Each of these eight filter channels are sequentially sampled for 40.9 seconds by an eight-position commutator as shown in Figure 3. This rapid sample detector makes it possible to study events that occur with a short time scale, for example, effects due to the rotation of the spacecraft.

In addition to the digital data available from the two spectrum analyzers, two broadband AGC receivers are used to produce detailed frequency-time spectrograms of narrow band and transient wave phenomena. A block diagram of the AGC receivers is shown in Figure 4. The receivers have the capability of operating in two different modes. The output of receiver no. 2 is a 13.5 kHz frequency modulated subcarrier with a bandwidth of 1 kHz. The output of receiver no. 1 can be either an 8.5 kHz frequency modulated subcarrier with a bandwidth of 1 kHz, or a direct mode which has a bandwidth from 650 Hz to 10 kHz.

A 20 kHz precision oscillator is used to convert data at frequencies from 11 kHz - 19 kHz and 21 kHz - 29 kHz to the frequency range covered by the direct mode.

The wideband receivers have eight different configurations that are obtained by different combinations of switching between the two spectrum analyzers and the four frequency ranges. The data researched for this report was usually recorded in the mode that cycles between the electric and magnetic antennas and the frequency ranges 650 Hz - 10 kHz, 11 kHz - 19 kHz, and 21 kHz - 29 kHz.

The IMP-6 University of Iowa plasma wave experiment has the versatility necessary for an experiment that operates in the wide range of environments found on the IMP-6 orbit. It is capable of obtaining data for the purpose of surveying naturally occurring radio noise and for studying specific events in detail. The excellent sensitivity of the spectrum analyzers used in conjunction with the long electric dipole antennas makes it possible to study a wide variety of electromagnetic and electrostatic wave phenomena in the magnetosphere, the magnetosheath, and the solar wind.

III. REVIEW OF PREVIOUS OBSERVATIONS

A. Upper Hybrid Resonance Noise

Naturally occurring band limited noise, called upper hybrid resonance noise, has been observed in the ionosphere and plasmasphere by several rocket- and satellite-borne experiments [Walsh et al., 1964; Bauer and Stone, 1968; Gregory, 1969; Muldrew, 1970; Hartz, 1970; and Mosier et al., 1973]. As reported by Mosier et al. [1973] upper hybrid resonance noise consists of waves with frequencies between the local upper hybrid resonance frequency, f_{UHR}, and the local plasma frequency, f_p. Less intense noise is also observed at frequencies between the plasma frequency and the L = 0 cutoff frequency, $f_{L=0}$.

$$f_{UHR} = (f_p^2 + f_g^2)^{1/2} \tag{1}$$

$$f_p = \frac{1}{2\pi} \left(\frac{e^2 n}{m\epsilon_o}\right)^{1/2} \tag{2}$$

$$f_g = \frac{1}{2\pi} \frac{eB}{m} \tag{3}$$

$$f_{L=0} = \left(f_p^2 + \frac{f_g^2}{4}\right)^{1/2} - \frac{f_g}{2} \tag{4}$$

where n is the electron number density and B is the static magnetic field. These resonance and cutoff frequencies define bounding surfaces

between which modes of wave propagation exist in a cold plasma with a variable number density and static magnetic field [see Stix, 1962].

The index of refraction for waves between f_{UHR} and the greater of f_g and f_p approaches infinity at the resonance cone angle, θ_{res}, measured with respect to the static magnetic field. The resonance cone angle varies from 90° when the wave frequency equals f_{UHR} to 0° when the wave frequency equals the greater of f_g or f_p. Waves that have wave vectors exactly at the resonance cone angle are purely electrostatic because the wave magnetic field approaches zero as the index of refraction approaches infinity. Wave energy can be generated by Cerenkov radiation from low energy electrons at wave normal angles near the resonance cone angle because the wave phase velocity can be less than the electron velocities for large values of the index of refraction.

Taylor and Shawhan [1974] have performed detailed numerical calculations of electric field and magnetic field wave spectral densities to test incoherent Cerenkov radiation as the mechanism responsible for generating various types of magnetospheric emissions. Taylor [1973] calculates wave electric field spectral densities for upper hybrid resonance noise that are several orders of magnitude greater than those typically measured; therefore, sufficient power is available from incoherent Cerenkov radiation for the generation of upper hybrid resonance noise. Smaller electric fields may be observed because of thermal effects, which were not taken into account in the calculations [see Taylor, 1973].

In summary, upper hybrid resonance noise consists of naturally occurring emissions in the frequency interval between the local upper hybrid resonance frequency and the greater of the plasma frequency or the electron gyrofrequency. Incoherent Cerenkov radiation from low energy electrons in the plasmasphere or ionosphere may generate upper hybrid resonance noise, and the propagation of the wave energy appears to be adequately described by cold plasma theory [see Mosier et al., 1973, Taylor and Shawhan, 1974.]

B. $(n + 1/2)f_g$ Harmonics

Intense narrow band electrostatic emissions, called $(n + 1/2)f_g$ harmonics, have been detected in the outer magnetosphere ($4 \leq L \leq 10$) by the OGO 5 spacecraft [Kennel et al., 1970; Fredricks and Scarf, 1973]. These emissions occur at frequencies between harmonics of the electron gyrofrequency, most often near $3/2\ f_g$. The $(n + 1/2)f_g$ harmonics have the greatest intensity and persistence near the geomagnetic equator and local midnight. They occur with electric field amplitudes typically from 1-10 millivolts per meter and have been observed with amplitudes as great as 100 millivolts per meter in association with geomagnetic substorms [Scarf et al., 1973].

Kennel et al. [1970] suggested that these emissions could be responsible for pitch angle diffusion and energization of auroral electrons. Detailed calculations of diffusion coefficients for scattering in energy and pitch angle show that these waves could cause such scattering for electrons in the energy range 0.1 - 10 keV [Lyons, 1974].

A mechanism has been proposed by Fredricks [1971] and later refined by Young et al. [1973] to explain the generation of the $(n + 1/2)f_g$ harmonics. This mechanism is an electrostatic plasma instability that is driven by an unstable velocity distribution function. The electron velocity distribution function used by Young et al. [1973] assumes the coexistence of both a warm species of electrons and a cold species. In addition, the warm species has a peak at some non-zero velocity in the distribution of the velocity component perpendicular to the static magnetic field, $V_\perp$. Similar peaks in the electron velocity distribution function of $V_\perp$ have been observed in the warm plasma associated with the plasma sheet [DeForest and McIlwain, 1971]. This unstable velocity distribution function provides the energy necessary to drive these electrostatic instabilities [see Young et al., 1973].

In summary, the $(n + 1/2)f_g$ harmonics are intense narrow band emissions that occur most often near $3/2\ f_g$ in the outer magnetosphere. These harmonics occur with the largest amplitudes near the geomagnetic equator and cannot be understood in terms of cold plasma theory. Instead, a generation mechanism has been proposed that requires a warm electron species with an unstable $V_\perp$ velocity distribution function coexisting with a low density background of cold electrons.

C. Trapped $f > f_p$ Electromagnetic Noise

Weak electromagnetic noise, called $f > f_p$ electromagnetic noise, has been observed in the outer magnetosphere by the University

of Iowa IMP 6 plasma wave experiment [Gurnett and Shaw, 1973]. This noise exists at frequencies above the local plasma frequency, and, in some cases, it provides a definite indication of the local plasma frequency [see Gurnett and Frank, 1974]. For these cases the noise has a sharp lower frequency cutoff at the local plasma frequency and nulls at twice the spacecraft spin rate, which indicate that the wave electric field vector is parallel to the static magnetic field.

Cold plasma theory allows the existence of two high frequency electromagnetic modes (called the ordinary mode and the extraordinary mode in ionospheric research) for a two component magnetized plasma. One of these modes is bounded by the surface at which the wave frequency equals the local plasma frequency, f_p, and the other is bounded where the wave frequency equals the R = 0 cutoff frequency, $f_{R=0}$

$$f_{R=0} = \left(f_p^2 + \frac{f_g^2}{4}\right)^{1/2} + \frac{f_g}{2} \qquad (5)$$

[see Stix, 1962]. Examples of $f > f_p$ noise are found with distinct lower frequency cutoffs at both the local plasma frequency and the R = 0 cutoff frequency. The identification of both cutoffs suggests that the noise consists of electromagnetic waves propagating in both the ordinary and the extraordinary modes. Since the waves that make up the $f > f_p$ noise are reflected from boundaries where the wave frequency equals the local plasma frequency (or the R = 0 cutoff frequency), the $f > f_p$ noise is trapped in the low density region between the plasmapause and the magnetopause [see Gurnett and Shaw, 1973]. This

electromagnetic radiation has been extensively studied, and it has recently been called non-thermal continuum radiation because of its broad frequency spectrum and nearly constant amplitude [Gurnett, 1975].

In summary, the $f > f_p$ noise consists of weak electromagnetic noise in the outer magnetosphere from which the local electron plasma frequency can sometimes be accurately determined. As for the upper hybrid resonance noise, the propagation characteristics of these waves appear to be described by the dispersion relations obtained from cold plasma theory.

IV. ELECTROSTATIC NOISE BANDS OBSERVED BY IMP 6

A. Identifying Characteristics

A portion of the spectrum analyzer data from a typical IMP 6 magnetospheric pass is shown in Figure 5. The data shown were recorded as the spacecraft moved outward from about 2.0 earth radii to about 10.0 earth radii geocentric radial distance. The data presented are the raw voltage outputs of the two spectrum analyzers (proportional to the logarithm of the signal amplitude), one of which is connected to the E_y electric dipole antenna, and the other of which is connected to the M_y magnetic loop antenna. The dynamic range of each frequency channel (100 db) is represented by the distance from the baseline of one channel to the baseline of the next channel. Each vertical bar represents the time-average electric (or magnetic) field strength measured over a time interval of 81.8 seconds, and the dots immediately above each bar represent the peak field strength seen over the same time interval.

The large signal strengths seen in the lowest frequency channels of the electric field data are interference that is produced when the loop antenna boom assembly shadows the spacecraft solar array panels. As the spacecraft spins the shadow of the loop antennas produces voltage transients on the solar array panels and the associated connecting wiring. This causes interference that is picked up by the plasma wave

experiment, particularly at low frequencies. The magnitude of this interference, which we call solar array interference, is dependent upon the properties of the plasma surrounding the spacecraft. Specifically, when the spacecraft crosses the plasmapause its strength is observed to increase greatly. This effect is seen at about 0300 UT in the electric field data shown in Figure 5.

A second indication of the plasmapause location is shown in the magnetic antenna filter channel data of Figure 5. A strong hiss band is observed from about 0130 - 0300 UT covering the frequency range from about 200 Hz to 3 kHz with an abrupt termination at approximately 0300 UT. This hiss, called plasmaspheric hiss, has been shown to be confined to the interior of the plasmasphere and terminates close to the location of the plasmapause [Russell et al., 1969; Russell and Holzer, 1970; Thorne et al., 1973]. Plasmaspheric hiss is observed on most IMP 6 passes through the plasmasphere, and the termination of the hiss and the increase in magnitude of the solar array interference provide a definite indication that the plasmapause has been crossed.

The inset in Figure 5 shows an electrostatic noise band of the type that are frequently found on IMP 6 passes through the magnetosphere. The noise band first becomes evident in the electric dipole antenna data at about 0220 UT in the 178 kHz filter channel. No corresponding signals are observed in the magnetic loop antenna data. The center frequency of the noise band decreases systematically as the radial distance of the spacecraft increases with an abrupt decrease

from 100 kHz to 16.5 kHz near the plasmapause crossing at about 0300 UT.

This abrupt decrease in frequency suggests that the frequency of the noise band may be related to the electron number density, which also decreases abruptly at the plasmapause. Therefore, the most likely resonance frequencies that could be associated with this noise band are the electron plasma frequency, f_p, and the upper hybrid resonance frequency, f_{UHR}, as defined by Equations (1) and (2). Both the plasma frequency and the upper hybrid resonance frequency change abruptly at the plasmapause similar to the change in frequency of the electrostatic noise band shown in Figure 5.

In addition, the center frequency of this noise band is typical of the electron plasma frequency in this region of the magnetosphere. Center frequencies of 100 kHz and 16.5 kHz, for example, would correspond to electron number densities of 120 cm^{-3} and 3.3 cm^{-3}, respectively. The noise band occurs at these frequencies near the inside and outside edges of the plasmapause, and these electron number densities are typical of those measured near the plasmapause [Carpenter et al., 1969; Harris et al., 1970].

Electrostatic noise bands of this type are observed on about two-thirds of all IMP 6 magnetospheric passes with characteristics similar to the example shown in Figure 5. The bands are most easily identified during quiet geomagnetic periods ($K_p \leq 2$). The characteristic variation in frequency with radial distance (as shown in

Figure 5) can be easily recognized on magnetospheric passes when K_p has low values. During more disturbed geomagnetic periods these bands either do not exist, or they are hidden by other types of noise which have greater amplitudes than those of the electrostatic noise bands.

B. Region of Occurrence

Since the frequency of these noise bands increases as the spacecraft moves to lower radial distances in the plasmasphere, it is probable that such bands occur at frequencies greater than 178 kHz (the upper spectrum analyzer filter channel) at lower altitudes in the plasmasphere. At larger altitudes, beyond the plasmapause, these noise bands are observed to decrease in bandwidth and intensity until, beyond about ten earth radii, they are no longer observed even though IMP 6 samples radial distances to about thirty earth radii. Thus, these bands are observed in the interior of the magnetosphere and probably extend to lower altitudes in the plasmasphere where upper hybrid resonance noise has been observed.

A survey was made of the location of all such electrostatic noise bands that were observed during the first year of operation of the IMP 6 plasma wave experiment. These noise bands were observed at all magnetic latitudes sampled by the IMP 6 orbit ($|\lambda_m| \leq 45°$).

Figure 6 shows the locations at which electrostatic noise bands of the type shown in Figure 5 were observed in the 31.1 kHz spectrum analyzer filter channel as a function of local time and radial distance.

The data plotted are the points at which the greatest intensity was measured at 31.1 kHz for all bands observed during the first year of operation of the experiment. Since the major axis of the orbit moves through one rotation in local time per year, this represents a nearly equal sampling of all local times. The peak response in the 31.1 kHz channel occurs at radial distances of four to five earth radii and shows a tendency to occur at larger radial distances near local evening than near local morning. The noise bands occur at all local times, least often in the quadrant from eighteen to twenty-four hours.

Figure 6 also shows the average location of the plasmapause in the equatorial plane as determined by data collected by the OGO 5 spacecraft [Chappell et al., 1971]. The peak response in the 31.1 kHz channel is observed at radial distances near that of the average plasmapause. The noise bands also have a tendency to be observed at greater radial distances near local evening, as does the plasmapause. (Almost all of the bands observed near local evening were observed at latitudes well off the equatorial plane ($20° < \lambda_m < 40°$) at which the plasmapause is located one to three earth radii lower than at the magnetic equator.) The tendency of these bands to occur near the plasmapause further supports the association of these bands with the local plasma frequency, since 31.1 kHz is typical of the plasma frequency near the plasmapause.

C. Spectral Characteristics

Electrostatic noise bands of the type shown in Figure 5 appear to occur as two distinct spectral types in the wideband spectrograms.

The first type appears in the spectrograms as one or more narrow, well defined lines, with bandwidths of a few hundred Hz. We have called this spectral type "narrow band electrostatic noise" because of its appearance in the wideband spectrograms. The second type, which we call "diffuse electrostatic noise", consists of one or more bands, generally a few kHz in width, often with a sharp upper frequency cutoff. The diffuse electrostatic noise frequently has nulls occurring at twice the spacecraft spin rate, and the narrow band electrostatic noise does not have spin modulated intensity.

An example of narrow band electrostatic noise is shown in Figures 7 and 8. The data shown in Figure 7 illustrate the frequencies at which the narrow band electrostatic noise is observed by the wideband receiver and the upper four spectrum analyzer filter channels. The open circles represent the time at which the largest signal strength was seen in each spectrum analyzer filter channel, and the horizontal bars represent the time interval during which any signal was present in that channel. The data shown were recorded from the E_y dipole antenna during an inbound magnetospheric pass, orbit 18, from about nine earth radii to two earth radii near local noon.

The narrow band electrostatic noise is evident in the 178 kHz filter channel at about two earth radii. The frequency of the noise band sweeps down fairly uniformly with increasing radial distance until the plasmapause is reached near five earth radii. The center frequency decreases abruptly at the plasmapause, and the noise band is observable in the wideband receiver data just outside the plasmapause.

Spectrograms of the wideband receiver data corresponding to points labeled A, B, and C in Figure 7 are shown in Figure 8. These high resolution spectrograms resolve the noise band into four distinct narrow bands which do not cross harmonics of the electron gyrofrequency as the spacecraft moves to larger radial distances beyond the plasmapause. (Values for harmonics of the electron gyrofrequency labeled f_g, $2f_g$, etc. in Figures 7 and 8 were calculated from simultaneous measurements of the geomagnetic field strength by the NASA/GSFC magnetometer experiment on IMP 6).

The lowest frequency band is found in the frequency interval bounded by the fourth and fifth harmonics of the electron gyrofrequency, and it extends to radial distances slightly beyond the plasmapause. A second band is found between the fifth and sixth harmonics of the electron gyrofrequency, and it extends to a radial distance of about eight earth radii. This noise band decreases in frequency at a rate slightly less than the rate of decrease of the harmonics of the electron gyrofrequency as can be seen in Figure 7. A third band is found between the sixth and seventh harmonics of the electron gyrofrequency from about seven to nine earth radii. A fourth band is found between the seventh and eighth harmonics near eight earth radii.

At about 0620 UT, marked by the label B in Figures 7 and 8, the noise bands are observed coincidentally with some trapped $f > f_p$ electromagnetic noise that is visible in the wideband spectrograms for several minutes. Nulls occurring at twice the spacecraft spin rate are visible in the wideband spectrogram of the $f > f_p$ electro-

magnetic noise shown in Figure 8. These nulls indicate that the wave electric field vector is polarized parallel to the geomagnetic field as would be expected for waves near the local plasma frequency. Thus, for the time period near 0620 UT the plasma frequency can be positively identified from this sharp lower frequency cutoff [see Gurnett and Shaw, 1973].

The narrow band electrostatic noise at 0620 UT occurs between consecutive harmonics of the electron gyrofrequency that are immediately above and immediately below the plasma frequency. Thus, the plasma frequency appears to strongly influence the frequency at which the bands occur at larger radial distances in the magnetosphere as well as near the plasmapause boundary.

The wideband receiver data in the spectrograms of Figure 8 also show that the narrow band electrostatic noise does not have nulls that occur as the spacecraft spins as does the $f > f_p$ electromagnetic noise. The nulls near the lower cutoff frequency of the $f > f_p$ noise are a result of the definite orientation of the wave electric field vector parallel to the geomagnetic field. Since such nulls are not observed for the narrowband electrostatic noise it is concluded that the wave electric field vector of the narrow band electrostatic noise is not strongly oriented either parallel to or perpendicular to the geomagnetic field.

Another IMP 6 magnetospheric pass, orbit 78, illustrating the second spectral type, which we call diffuse electrostatic noise, is shown in Figures 9 and 10. The wideband receiver data show that the

diffuse electrostatic noise consists of three distinct bands. The center frequencies of these noise bands are bounded in frequency by consecutive harmonics of the electron gyrofrequency at radial distances beyond the plasmapause as were the center frequencies of the narrow band electrostatic noise. The bands between the second and third harmonics and between the third and fourth harmonics are observed to have a sharp upper frequency cutoff while the band between the first and second harmonics has no distinct upper cutoff.

Wideband spectrograms of the noise bands at points labeled A, B, and C in Figure 9 are shown in Figure 10. As is shown in spectrogram A the bands are observed to have nulls that occur at twice the spin rate of the spacecraft. The position of these nulls indicates that the wave electric field vector of the diffuse electrostatic noise is oriented perpendicular to the geomagnetic field direction. All values of the geomagnetic field used in this paper were measured by the NASA/GSFC magnetometer experiment onboard IMP 6, with the exception of those specifically labeled as "predicted", for example, from 0300 - 0405 UT in Figure 9 which were computed from the Jensen-Cain expansion for the geomagnetic field.

The plasma frequency can be identified at large radial distances by the sharp lower frequency cutoff of the $f > f_p$ electromagnetic noise as shown in spectrogram C of Figure 10. The diffuse electrostatic noise on orbit 78 is seen to occur between harmonics of the electron gyrofrequency that are near the local electron plasma frequency, similar to the narrow band electrostatic noise observed on orbit 18.

Near 0505 UT as shown in Figure 9, the noise band between $3f_g$ and $4f_g$ develops a sharp lower frequency cutoff. Nulls at twice the spacecraft spin rate occur at both the upper and lower frequency cutoffs which indicate that the wave electric field vector is parallel to the geomagnetic field at the lower frequency cutoff and perpendicular to the geomagnetic field at the upper cutoff. Because of the orientation of the wave electric field and the frequency at which the lower cutoff occurs relative to the lower frequency cutoff of the trapped electromagnetic noise (see Figure 9) it is reasonable to believe that the lower cutoff frequency of this diffuse noise band is equal to the local plasma frequency. A few other cases of diffuse electrostatic noise have a sharp lower frequency cutoff similar to the example shown in Figures 9 and 10, however, this sharp lower cutoff is not usually observed.

Narrow band electrostatic noise and diffuse electrostatic noise are not often observed on the same magnetospheric pass; however, in a few cases they are observed simultaneously. The narrow band electrostatic noise has a tendency to be observed between harmonics greater than $3f_g$, and the diffuse electrostatic noise is most often observed between harmonics below $3f_g$. The diffuse electrostatic noise is most often observed near the plasmapause while the narrow band electrostatic noise tends to extend to larger radial distances in the outer magnetosphere. Both types of noise can exist continuously for distances of several earth radii beyond the plasmapause.

D. Wave Electric Field Strength and Associated Wave Magnetic Field Strength

Figure 11 shows the distribution of electric field spectral densities that were measured for all noise bands of the type shown in Figure 5 during the first year of operation of the University of Iowa experiment. These data represent the largest signal strength for the bands in the 31.1 kHz spectrum analyzer filter channel.

Values for the electric field spectral densities were calculated by assuming the wave electric field to be equal to the voltage measured at the antenna divided by one-half the tip-to-tip length of the antenna. In addition, the noise bands were assumed to have a bandwidth larger than the effective spectrum analyzer filter bandwidth to calculate values for spectral density. This assumption is valid for most cases of diffuse electrostatic noise, however, it is not valid for the narrow band electrostatic noise because it typically has a bandwidth of about one-tenth that of the spectrum analyzer filter channels. The error introduced by this assumption could cause the actual spectral densities of the narrow band electrostatic noise to be a factor of about ten larger than those shown in Figure 11. Since this is not a large error in terms of the ranges of the data (10^8 in spectral density) no attempt was made to correct values of spectral density for the narrowband electrostatic noise.

Either narrow band electrostatic noise or diffuse electrostatic noise was observed on about two-thirds of the total number of magnetospheric passes during the first year of operation of the IMP 6 experiment. The noise bands occur most often with a peak wave electric

field spectral density near 10^{-15} volts^2 meter^{-2} Hz^{-1} corresponding to a broadband field amplitude of about two microvolts per meter. It is uncertain whether the low occurrence of bands shown near a spectral density of 10^{-16} volts^2 meter^{-2} Hz^{-1} is due to less relative occurrence or masking due to variations in the background levels of other types of waves received by the antenna, for example, the $f > f_p$ electromagnetic radiation.

In most cases of these types of noise bands no wave magnetic field was observed, however, there was an observable wave magnetic field component in the digital spectrum analyzer data for eight out of the approximately 110 noise bands investigated. These eight cases are examined in Figure 12. For each occurrence the peak electric field energy density of the bands is plotted as a function of the peak magnetic field energy density. The peak signal strength plotted represents the largest signal observed in the 31.1 kHz filter channel during the time interval over which the noise band was observed in that filter channel.

As can be seen in Figure 12, the peak electric field energy density of the noise bands is typically about four orders of magnitude larger than the peak magnetic field energy density, and these eight cases are associated with unusually intense values of wave electric field strength. Seven of these eight cases had values of electric field spectral density in excess of 10^{-11} volts^2 meter^{-2} Hz^{-1}. There were five other cases of noise bands with peak electric field spectral

densities between 10^{-11} volts^2 meter^{-2} Hz^{-1} and 10^{-8} volts^2 meter^{-2} Hz^{-1} for which no associated wave magnetic field was observed. All but one of these twelve cases of the most intense noise bands were observed near the dayside of the plasmapause.

It is not possible to determine experimentally if the weaker noise bands (electric field spectral densities below 10^{-12} volts^2 meter^{-2} Hz^{-1}) have wave magnetic fields with energy densities four orders of magnitude less than their electric field energy densities. If these bands do have a proportionally weak wave magnetic field they could not be detected with the magnetic antenna on IMP 6.

The relationship between the wave magnetic field strength and the wave electric field strength has been investigated in detail for one specific pass, the inbound portion of orbit 14. On this pass noise bands were observed with a particularly intense wave electric field and a detectable wave magnetic field. Figure 13 shows the raw voltage outputs from the upper six spectrum analyzer channels on this pass. At least two distinct noise bands can be distinguished sweeping upward in frequency as the spacecraft approaches the plasmapause at about 1820 UT. These noise bands are particularly intense in the 31.1 kHz electric field channel, and a weak but clear response is evident at corresponding times in the 31.1 kHz magnetic field channel.

The electric antenna, E_x, wideband receiver data shown in Figure 14 resolves these bands into five distinct noise bands. The three lowest frequency bands have spectral characteristics similar to the diffuse electrostatic noise while the upper two bands are

characteristic of the narrow band electrostatic noise. Also plotted in Figure 14 are the points at which signals are observed in the magnetic antenna, M_y, spectrum analyzer data. The wave magnetic field is first evident in the 31.1 kHz spectrum analyzer filter channel (above the upper frequency limit of the wideband receiver, 29 kHz). No signals were observed in the magnetic antenna wideband receiver data, therefore, it is not possible to determine if the wave magnetic field is associated with only one of the spectral types of noise or with both types.

Figure 15 shows a plot of the corresponding electric and magnetic field spectral densities measured by the peak detector of the 31.1 kHz filter channel as the spacecraft passed through the region containing these noise bands. The 5.11 second samples of magnetic field spectral density in Figure 15 were calculated by subtracting the noise level spectral density of the magnetic receiver in order to reduce the error caused by the preamplifier noise at small signal levels. The peak wave magnetic field intensity of these bands is not simply proportional to the peak electric field intensity, although there is a clear tendency for the magnetic field strength to increase as the electric field strength increases.

It is not possible to experimentally determine the phase velocity of the electromagnetic component of the waves shown in Figures 13 and 14. The phase velocity of any electromagnetic wave is equal to the magnitude of the component of the wave electric field transverse to the wave vector direction divided by the magnitude of the wave

magnetic field [see Allis, et al., 1963]. This experiment measures the peak value of the wave electric and magnetic field components in the plane of rotation of the spacecraft. If there is a wave electric field component in the direction of the wave vector it is not necessarily possible to distinguish it from the transverse component of the electric field vector.

In the case of upper hybrid resonance noise, for example, noise can be generated by incoherent Cerenkov radiation from low energy electrons because near the resonance cone angle the wave phase velocity is less than the electron velocities. The ratio of the magnitude of the total electric field to the magnitude of the magnetic field is large, however, because there is a large electric field component in the direction of the wave vector. This electric field component results from the resonance with the plasma, and this component of the wave electric field is electrostatic.

Taylor [1973] has calculated values for the electric field and magnetic field spectral densities generated by incoherent Cerenkov radiation on the frequency interval between f_{UHR} and the greater of f_p or f_g. These calculations were performed near the geomagnetic equator just inside the plasmapause at wave frequencies of 100 kHz and 178 kHz. These calculations result in a value of 1000 for the magnitude of the total wave electric field divided by the product of the speed of light and the magnitude of the wave magnetic field.

This ratio, E/cB, for the noise bands shown in Figure 15 is plotted as a function of Universal Time, UT, in Figure 16. The

vertical error bars in Figure 16 indicate the precision of the magnetic field measurement as affected by the digitizing step size and the subtraction of the magnetic receiver noise level spectral density. The precision is smallest at low signal levels as is evident for the smallest values of magnetic field spectral density shown in Figure 15.

Figure 16 shows that the wave electric field amplitude of these noise bands ranges between 4 and 150 times greater than that expected for an electromagnetic wave in free space as compared to the wave magnetic field amplitude (E = cB for electromagnetic waves in free space). In addition, the value of E/cB for these noise bands is one to two orders of magnitude less than that computed by Taylor [1973].

The spectral characteristics of these type of noise bands (as shown in Figure 7, Figure 9, and Figure 14) outside the plasmapause are clearly different than those calculated by Taylor [1973] using the cold plasma dispersion relation. These noise bands have been shown to closely track changes in the electron gyrofrequency, they are not constrained to the frequency interval between f_{UHR} and the greater of f_p or f_g, and they often occur with narrow bandwidths, which is untypical of most types of noise that have been attributed to incoherent Cerenkov radiation. It is apparent that the warm plasma population found in the plasma sheet must be considered to explain the observed characteristics of these emissions.

Additional evidence supporting the argument that the warm plasma sheet electron population is necessary to generate these noise bands is found in Figure 6. The average radial distance at which the

noise bands at 31.1 kHz occur is about one earth radii greater in the pre-midnight local time sector than in the post-midnight sector. The relationship between the plasmapause and the plasmasheet near local midnight has been examined using data collected by the OGO 3 satellite [Frank, 1971].

The pre-midnight sector differs from the post-midnight sector in that the earthward edge of the plasma sheet is found one to three earth radii beyond the plasmapause before local midnight while in the post-midnight sector the plasmapause location is nearly coincident with the earthward edge of the plasma sheet. The region between the plasmapause and the earthward edge of the plasma sheet is characterized by a region of low electron energy density called the electron trough [see Frank, 1971]. The observed change in the location of the electrostatic noise bands in crossing local midnight is comparable to the change in position of the earthward edge of the plasma sheet. This is consistent with the suggestion that the generation of these noise bands must be dependent on the presence of the warm plasma sheet electron population.

In summary, the following observations have been made concerning the wave magnetic field that is occasionally observed in association with these noise bands. First, the wave magnetic field is only observed for unusually intense cases of electric field strength, and it is not always observed for all such cases. Second, the energy density of the wave magnetic field is one to four orders of magnitude lower than the wave electric field energy density. Finally, although there

is a tendency for the wave magnetic field strength to increase as the electric field strength increases, there appears to be no well defined proportionality between the wave electric field strength and the wave magnetic field strength as there is for electromagnetic waves well above the plasma frequency [for example, see Gurnett and Shaw, 1973 and Gurnett, 1974].

We have chosen to refer to these bands as electrostatic noise bands because the dominant wave energy is contained in the wave electric field, and because a wave magnetic field is infrequently and inconsistently observed. In addition, theories of electrostatic instabilities predict electrostatic noise at frequencies between harmonics of the electron gyrofrequency [Fredricks, 1971; Young et al., 1973], and these noise bands occur with characteristics similar to those electrostatic instabilities. The wave magnetic field could be a result of coupling between these electrostatic modes and other electromagnetic modes of propagation, or it could be caused by electromagnetic resonances that have characteristics similar to the electrostatic resonances but with an associated wave magnetic field. Cheng [1975] has calculated dispersion characteristics and growth rates for electromagnetic instabilities propagating perpendicular to the static magnetic field, however, no instability analysis has been done for modes propagating along the field at the time of writing of this report.

V. RELATIONSHIP TO UHR NOISE AND $(n + 1/2)f_g$ HARMONICS

Near the plasmapause the diffuse electrostatic noise frequently has characteristics that are similar to the upper hybrid resonance noise observed at lower altitudes in the ionosphere and plasmasphere. Figure 17 shows an example of the diffuse electrostatic noise that has characteristics similar to the upper hybrid resonance noise. This noise band is observed near the plasmapause, and the diffuse electrostatic noise develops a sharp lower cutoff similar to the example previously discussed in Figure 9. The noise band has a sharp upper frequency cutoff, and it develops a sharp lower frequency cutoff at 1617 UT near 5.0 earth radii. At 1625 UT and 1628 UT near 4.7 earth radii the lower frequency cutoff has become well defined, and intensity modulations at twice the spacecraft spin rate are observed. At 1648 UT the lower frequency cutoff is no longer observed.

The position of the maxima in the spin modulation of the noise band indicates that the wave electric field vector is aligned parallel to the geomagnetic field at the lower cutoff frequency. Waves occurring at frequencies near the local plasma frequency would be expected to have an electric field that is aligned parallel to the geomagnetic field. Because of the alignment of the wave electric field vector, and the similarity of this example to the one discussed

in Figure 9, it is reasonable to conclude that the lower cutoff frequency is equal to the local plasma frequency.

The local plasma frequency (defined by the sharp lower cutoff of the noise band), the electron gyrofrequency (measured by the NASA/GSFC magnetometer experiment on IMP 6), and the upper hybrid resonance frequency (calculated from Equation 1) have been indicated next to the wideband spectrograms shown in Figure 17. The calculated upper hybrid resonance frequency occurs near to, but not at, the sharp upper cutoff frequency of the diffuse electrostatic noise. It was this close correspondence observed for several examples of the diffuse electrostatic noise which initially led to the incorrect conclusion that the diffuse electrostatic noise was upper hybrid resonance noise observed beyond the plasmapause with the upper cutoff frequency equal to the local upper hybrid resonance frequency [see Shaw and Gurnett, 1972].

As the examples discussed in this paper have shown, these noise bands are constrained to frequencies bounded by consecutive harmonics of the electron gyrofrequency at radial distances outside the plasmasphere. In addition, the positive identification of the local plasma frequency from the sharp lower frequency cutoff of the $f > f_p$ noise conclusively shows that these bands cannot have an upper cutoff frequency equal to the local upper hybrid resonance frequency [see Gurnett and Shaw, 1973].

The diffuse electrostatic noise does appear to be related to the upper hybrid resonance noise observed at lower altitudes in the

following sense, however. Mosier et al. [1973] reports an example of upper hybrid resonance noise observed well inside the plasmasphere with the IMP 6 GSFC radio astronomy experiment on an inbound magnetospheric pass on orbit 15 at frequencies of several hundred kHz (well above the upper frequency channels of the University of Iowa experiment). Figure 1 of Mosier et al., [1973] shows that this noise continues downward in frequency to frequencies as low as thirty kHz as the spacecraft moves from the interior of the plasmasphere towards the plasmapause. Examination of the University of Iowa plasma wave experiment data from orbit 15 confirms that the upper hybrid resonance noise observed by Mosier et al. develops into the electrostatic noise bands observed by the University of Iowa experiment outside the plasmapause. However, outside the plasmapause these noise bands are strongly controlled by the harmonics of the electron gyrofrequency and are no longer related to the local upper hybrid resonance frequency.

At larger radial distances in the magnetosphere intense narrow band harmonics that are similar to the $(n + 1/2)f_g$ cyclotron harmonics observed by Kennel et al. [1970] are found in the IMP 6 data. An example of these type of harmonics observed on orbit 36 near seven earth radii is shown in Figure 18. These harmonic emissions have spectral characteristics more similar to those reported by Kennel et al. [1970] and Fredricks and Scarf [1973] than do the diffuse electrostatic noise bands and the narrow band electrostatic noise. These harmonic emissions tend to disappear and reappear in the spectrograms

with time scales of the order of a few minutes while the electrostatic noise bands reported in this paper exist continuously in the wideband spectrograms for periods of tens of minutes to hours. In addition, the $(n + 1/2)f_g$ harmonics typically have broadband electric field strengths about three orders of magnitude greater than those typical of the diffuse and narrow band electrostatic noise [Kennel et al., 1970].

In many cases regions containing diffuse electrostatic noise and narrow band electrostatic noise have been observed to merge smoothly into regions containing the type of harmonic emission shown in Figure 18, which is probably the $(n + 1/2)f_g$ harmonics previously observed in the outer magnetosphere. This merging appears to be a process which occurs over several earth radii as the spacecraft moves outward from the plasmapause during which the spectral characteristics of the electrostatic noise bands change to those more characteristic of the $(n + 1/2)f_g$ harmonics. Thus, the electrostatic noise bands appear to be related to the $(n + 1/2)f_g$ harmonics as well as the upper hybrid resonance noise.

This merging process is undoubtedly explained by changes in the plasma characteristics in the different regions of the magnetosphere containing these different types of emissions. Electron number densities inside the plasmasphere are large (~ 1000 cm^{-3}) and temperatures are low (~ 1 eV). Moving out through the plasmapause and into the plasma sheet we find an energetic particle population with low densities and high temperatures ($n_e \sim 1$ cm^{-3}, $T_e \sim 1$ keV). Near the plasmapause there must occur a transition between these regions in which some

combination of cold plasmaspheric electrons and warm plasma sheet electrons may exist.

At large radial distances in the outer magnetosphere the generation of the $(n + 1/2)f_g$ harmonics may be explained by electrostatic instabilities the nature of which are determined primarily by the warm plasma population with a lower background density of cold electrons as suggested by Young et al. [1973]. Moving towards the plasmasphere the cold electron population density increases while the warm electron population density decreases until, inside the plasmasphere the warm plasma sheet population has disappeared and the electrostatic instabilities are no longer generated. Instead, noise is generated between the local upper hybrid resonance frequency and the greater of f_p or f_g by incoherent Cerenkov radiation from low energy electrons. The propagation of this noise would be characteristic of the cold plasma dispersion relation, and it would be observed as upper hybrid resonance noise.

The electrostatic noise bands observed by the University of Iowa IMP 6 plasma wave experiment usually occur during the transition between these two different regions of the magnetosphere (near the plasmapause). The continuous merging of these emissions with upper hybrid resonance noise and $(n + 1/2)f_g$ harmonics appears to represent a smooth transition between these types of noise as the spacecraft moves from the plasmasphere to the plasma sheet. It is suggested that this continuous merging can be explained by changes in the plasma characteristics that modify the generation and propagation of these types of naturally occurring magnetospheric emissions.

VI. SUMMARY OF EXPERIMENTAL RESULTS

The experimental observations of the electrostatic noise bands by the IMP 6 University of Iowa plasma wave experiment are summarized here:

(1) The noise bands are observed on about two-thirds of all IMP 6 passes through the magnetosphere. They are detected at all latitudes covered by the IMP 6 orbit ($|\lambda_m| \leq 45°$) and are found at all local times, least often in the quadrant from 18 to 24 hours local time.

(2) The noise bands consist of two spectral types, diffuse electrostatic noise and narrow band electrostatic noise. Diffuse electrostatic noise usually has a bandwidth of a few kHz. In some cases the noise has a sharp upper frequency cutoff, and in a few cases the noise has a sharp lower frequency cutoff that has been identified as the local plasma frequency. The wave electric field vector of the diffuse electrostatic noise is oriented perpendicular to the geomagnetic field direction. Narrow band electrostatic noise consists of sharp, well defined lines with a bandwidth of a few hundred Hz. The wave electric field vector of these waves is not strongly oriented either parallel to or perpendicular to the geomagnetic field direction.

(3) Both diffuse electrostatic noise and narrow band electrostatic noise occur at frequencies that are strongly controlled by the local

electron gyrofrequency. These types of noise track the electron gyrofrequency outside the plasmapause, and the noise bands are always bounded by consecutive harmonics of the electron gyrofrequency.

(4) The local plasma frequency also appears to have an influence on the frequencies at which these types of noise occur. The noise bands are observed to increase abruptly in frequency at the plasmapause, as does the local plasma frequency. In addition, the bands are often found between harmonics of the electron gyrofrequency that are near the local plasma frequency as identified by the sharp lower frequency cutoff of trapped $f > f_p$ noise.

(5) The noise bands are usually weak, having electric field spectral densities typically near 10^{-15} volts^2 meter^{-2} Hz^{-1} (broadband field strengths of about two microvolts per meter). The most intense cases of these noise bands have wave electric field spectral densities between 10^{-11} volts^2 meter^{-2} Hz^{-1} and 10^{-8} volts^2 meter^{-2} Hz^{-1}, and these intense cases were all observed near the dayside of the plasmapause.

(6) The most intense cases of the noise bands have been observed to have an associated wave magnetic field. The energy density of the wave magnetic field is one to four orders of magnitude less than the energy density of the wave electric field. Although the wave magnetic field tends to increase as the wave electric field increases, they are not related by a simple proportionality as are electromagnetic waves in free space, for example.

(7) These type of noise bands are contained with the magnetosphere. Inside the plasmasphere they are observed to connect smoothly with

upper hybrid resonance noise that has been observed at lower altitudes in the plasmasphere and ionosphere. As the spacecraft moves to larger radial distances in the outer magnetosphere the electrostatic noise bands often merge smoothly into regions containing emissions that are more characteristic of the $(n + 1/2)f_g$ harmonics previously observed in the outer magnetosphere. The electrostatic noise bands observed by the University of Iowa experiment have different characteristics than either of the upper hybrid resonance noise or the $(n + 1/2)f_g$ harmonics, however, they do represent a smooth transition between these two types of naturally occurring noise that are found in dissimilar regions of the magnetosphere.

Figure 19 is an idealized view of the dayside magnetosphere showing the locations and frequencies at which the different types of noise discussed in this report occur. The local plasma frequency, upper hybrid resonance frequency, and electron gyrofrequency are plotted as a function of geocentric radial distance.

Upper hybrid resonance noise is observed well inside the plasmasphere between f_{UHR} and f_p. This noise develops into the electrostatic noise bands observed by the University of Iowa experiment near the plasmapause. Diffuse electrostatic noise is most often observed at frequencies below 3 f_g, and narrow band electrostatic noise is most often observed at frequencies above 3 f_g. The electrostatic noise bands merge smoothly into regions containing the $(n + 1/2)f_g$ harmonics.

The $f > f_p$ electromagnetic noise, also called non-thermal continuum radiation, is observed at frequencies above the local plasma

frequency and consists of two components, a trapped component that is contained within the reflective boundaries formed by the plasmapause and the magnetopause and an escaping component that propagates into the solar wind [see Gurnett, 1975].

VII. DISCUSSION

Fredricks [1971] has proposed a theory refined by Young et al. [1973] to explain the generation of the $(n + 1/2)f_g$ harmonics observed in the outer magnetosphere. These electrostatic instabilities are generated by a non-Maxwellian electron velocity distribution consisting of a cold species coexisting with a warm species that has a peak at some non-zero velocity in the distribution of the velocity component perpendicular to the geomagnetic field.

Taylor and Shawhan [1974] have performed detailed calculations of the electric and magnetic field spectral densities caused by Cerenkov radiation from low energy plasmaspheric electrons at frequencies between the local plasma frequency and the upper hybrid resonance frequency. These calculations indicate that sufficiently large electric fields result from incoherent Cerenkov radiation to explain the generation of upper hybrid resonance noise.

The electrostatic noise bands observed by the IMP 6 University of Iowa plasma wave experiment show that these two different types of noise smoothly connect as the spacecraft moves from within the plasmasphere to the outer magnetosphere. Here we examine how such a smooth transition can occur between noise generated in regions of the magnetosphere that contain plasmas as dissimilar as those of the plasmasphere and the plasma sheet.

The dispersion relation for electrostatic modes in an infinite, homogeneous plasma with a constant magnetic field is the Harris [1959] dispersion relation shown in Equation (6).

$$0 = 1 + \sum_j \frac{\omega_{pj}^2}{k^2} \int d^3v \sum_{n=-\infty}^{\infty} \frac{J_n^2(k_\perp v_\perp/\omega_{gj})}{\omega - n\omega_{gj} - k_{||} v_{||}} \left[\frac{n\omega_{gj}}{v_\perp} \frac{\partial f_{oj}}{\partial v_\perp} + k_{||} \frac{\partial f_{oj}}{\partial v_{||}} \right] \tag{6}$$

The summation j is over all plasma species, ω is the angular wave frequency ($\omega = 2\pi f$), k is the wave vector, f_{oj} is the equilibrium velocity distribution function of the j^{th} species, and the subscripts $||$ and $\perp$ refer to the direction of the static magnetic field and the direction normal to the magnetic fied respectively.

The Harris dispersion relation can be evaluated for high frequency modes in a cold plasma by assuming that the ions are infinitely massive and by evaluating Equation (6) for a cold electron velocity distribution, f_c,

$$f_c = \frac{\delta(v_{||})\ \delta(v_\perp)}{2\pi v_\perp} \tag{7}$$

This results in the expression shown in Equation (8),

$$1 - \frac{\omega_p^2}{k^2} \left[\frac{k_\perp^2}{\omega^2 - \omega_g^2} + \frac{k_{||}^2}{\omega^2} \right] = 0, \tag{8}$$

which simplifies to

$$\tan^2\alpha = \frac{(f_p^2 - f^2)(f^2 - f_g^2)}{f^2(f^2 - f_{UHR}^2)} \qquad (9)$$

where $k_\perp = k \sin\alpha$ and $k_{||} = k \cos\alpha$. Equation (9) is identical to the expression for the resonance cone angle, θ_{res}, predicted by cold plasma theory [see Stix, 1962].

Wave energy generated by Cerenkov radiation from thermal electrons occurs at wave vector angles near the resonance cone angle for wave frequencies between f_{UHR} and the maximum of f_p or f_g. Thermal effects and collisions effectively prevent the index of refraction from reaching infinity, and the waves generated are electromagnetic ($|\vec{B}| \neq 0$). Therefore, Cerenkov emission consists of electromagnetic radiation that is generated near an electrostatic limit described by the Harris electrostatic dispersion relation shown in Equation (6).

The Harris dispersion relation has been used to examine various types of plasma instabilities that are driven by non-Maxwellian velocity distributions. These distributions usually fall into the category of temperature anisotropies [Harris, 1959], non-monotonic distributions of $v_\perp$ [Fredricks, 1971], and more complicated combinations of these two types of distributions [Young et al., 1973].

Young et al. have numerically evaluated the Harris dispersion relation for the Dory et al. [1965] loss-cone distribution defined as

$$f_{DGH}^{(j)}(v_\perp) = \frac{j^j}{\pi\alpha_\perp^2(j-1)!}\left(\frac{v_\perp}{\alpha_\perp}\right)^{2j}\exp\left[-j\left(\frac{v_\perp}{\alpha_\perp}\right)^2\right] \qquad (10)$$

where $f_{DGH}^{(j)}$ is peaked at $v_\perp = \alpha_\perp$. In addition to this warm species of electrons a low density background of cold electrons ($T_e \sim 1$ eV) is assumed to exist as an independent plasma constituent.

Electron velocity distributions that are sharply peaked at non-zero $v_\perp$ have been observed in the outer magnetosphere. DeForest and McIlwain [1971] and DeForest [1972] have published electron energy spectra that have sharply peaked $v_\perp$ distributions near a perpendicular velocity corresponding to an energy of about 100 eV. These spectra were obtained during magnetically disturbed periods when warm plasma is injected from the distant plasma sheet to altitudes below synchronous altitude (6.6 R_E) at which the ATS 5 spacecraft is located. A comparison of these measured energy spectra with the $f_{DGH}^{(j)}$ distribution shows that the sharp positive slope region at velocities less than the peak of the distribution can be steeper than that for $j = 5$.

A cold species of electrons in the plasma sheet usually can not be measured by satellite experiments; however, DeForest [1972] has obtained measurements of the density of this plasma constituent during satellite charging events associated with the substorm injection of warm plasma sheet electrons to lower altitudes in the magnetosphere. Because of the negative charging of the satellite, protons with energies below 50 eV (the lower limit of the ATS 5 measurements) are accelerated to the satellite and are measured by the experiment at higher total energies. DeForest estimates that the number density of the cold background plasma is about one per cent of the warm plasma

number density, which is typically near 1 cm^{-3} during the energetic plasma injection events.

Gurnett and Frank [1974] have compared measurements of the total plasma number density obtained from the lower frequency cutoff of the trapped $f > f_p$ electromagnetic noise with measurements of the number density of electrons with energies above 88 electron volts obtained from the low-energy proton and electron differential energy analyzer (LEPEDEA) experiment on IMP 6. These measurements, made on one IMP 6 outbound magnetospheric pass, showed that twenty to fifty per cent of the total proton number density consisted of protons with energies below 88 electron volts. For a part of this pass, essentially all the protons had energies greater than 88 electron volts, and the cold thermal constituent was not detectable. The thermal protons were estimated to have a temperature of about seven electron volts assuming the distribution to be a Maxwellian below the lower energy proton channels of the LEPEDEA experiment.

These measurements show that non-Maxwellian electron velocity distributions are often observed in the outer magnetosphere. Because the electrostatic noise bands observed by the University of Iowa experiment occur in the same regions of the magnetosphere that these anomalous electron velocity distributions are found, it is likely that electrostatic instabilities driven by these unstable distributions generate the noise observed by the plasma wave experiment. In addition, there are some similarities between the types of emissions discussed by Young et al. and the narrow band electrostatic noise and the diffuse electrostatic noise observed by the University of Iowa experiment.

Young et al. discuss two types of instabilities, "flutelike" modes for which $k_{||} = 0$, and modes which have a finite $k_{||}$. The "flutelike" modes require a sharp positive slope in the distribution of $v_{\perp}$ and a high warm plasma density for waves at frequencies near 3/2 f_g. For frequencies somewhat above 3/2 f_g, the required threshold density and the sharpness of the positive slope in $v_{\perp}$ decrease. In addition, increasing the ratio of the number density of the cold species to that of warm species, N_c/N_w, requires a smaller warm plasma threshold density to generate the instability.

Diffuse electrostatic noise has characteristics similar to those expected from the "flutelike" electrostatic modes. The diffuse electrostatic noise is found near the outside edge of the plasmapause boundary where N_c/N_w would be expected to be the largest. At larger radial distances in the magnetosphere the diffuse electrostatic noise is seldom found. Diffuse electrostatic noise is most often observed during quiet geomagnetic periods when N_c/N_w is expected to be larger at greater distances beyond the plasmapause, thus lowering the threshold electron density required for the instability to occur. Finally, diffuse electrostatic noise is seldom found at frequencies near or below 3/2 f_g. Most often the frequency is significantly higher than 3/2 f_g (see Figure 9, for example).

The data presented in Figure 9 at 0420 UT show the lowest frequency band of diffuse electrostatic noise between 1.5 f_g and 1.8 f_g. The measured electron gyrofrequency is 8.7 kHz and the plasma frequency is estimated to be equal to 21.4 kHz (by extending a straight

line from the lower cutoff of the $f > f_p$ noise at 0530 UT to the electrostatic noise in the 31.1 kHz filter channel at 0330 UT near the plasmapause).

Young et al. calculates values for threshold densities necessary to produce the electrostatic instability for the Dory loss-cone distribution (Equation (10)) for $j = 1$ and $j = 2$. If a value for the ratio of the cold electron species number density to the warm electron species number density is chosen, for example $N_c/N_w = 0.5$ (typical of the values given by Gurnett and Frank [1974]), then the threshold density and the frequency of the instability can be estimated (see Figures 4 and 5 of Young et al. [1973]).

For a value of $N_c/N_w = 0.5$ and $j = 1$ the instability occurs at $1.9\ f_g$ and a threshold density of $6.9\ cm^{-3}$ is required. For a value of $j = 2$ the instability occurs at $1.8\ f_g$ and a threshold density of $5.6\ cm^{-3}$ is required. Comparing this with the observed bandwidth of the noise, $1.5\ f_g$ to $1.8\ f_g$, and the estimated total number density, $5.6\ cm^{-3}$, we note that the electron density is high enough to generate the instability, but that the instability occurs only near the upper frequency limit of the noise band.

Lowering the ratio N_c/N_w lowers the frequency of the instability, however, it also raises the threshold density required to generate the instability. For example, if we choose $N_c/N_w = 0.1$, the instability is generated at $1.7\ f_g$ and $1.6\ f_g$ for $j = 1$ and $j = 2$ respectively. Threshold densities of $30.6\ cm^{-3}$ and $20.4\ cm^{-3}$ are required, however. While such high number densities are not impossible, they are somewhat

higher than those typically measured two earth radii beyond the plasmapause.

It is clear from this discussion that two criteria must be satisfied in order for the flutelike modes to be the generation mechanism for the diffuse electrostatic noise. First, the ratio N_c/N_w must be relatively high, most likely of the order of one-half or greater. Second, the positive slope region of the $v_\perp$ distribution must be sharper than the Dory loss-cone distribution defined by Equation (1) and evaluated for $j = 2$. Even under these conditions, the instability most likely would not occur at frequencies as low as $1.5\ f_g$.

The narrow band electrostatic noise observed by the University of Iowa experiment is generally observed at higher harmonic numbers than the diffuse electrostatic noise. Young et al. predict the existence of high frequency doublets and triplets separated by approximately the electron gyrofrequency for which $k_{||} \neq 0$. These modes are predicted to exist at frequencies only slightly above multiples of the electron gyrofrequency; however, bands are often observed well above the exact multiples (see the band between $4f_g$ and $5f_g$ in Figure 7, for example). According to Young, et al., the high frequency instabilities occur at higher frequencies as the ratio of the plasma frequency to the electron gyrofrequency increases. As the spacecraft moves into the outer magnetosphere the ratio f_p/f_g increases, and the narrow band electrostatic noise also has a tendency to occur at higher frequencies (note the band between $5\ f_g$ and $6\ f_g$ in Figure 7, for example).

The Harris dispersion relation does not explain the associated wave magnetic field that has been infrequently observed by the University of Iowa experiment. It is possible that the instabilities causing this noise are electromagnetic in nature with characteristics similar to the electrostatic limit. This is similar by analogy to incoherent Cerenkov radiation believed responsible for the generation of upper hybrid resonance noise. Such an electromagnetic instability, similar to those investigated by Cheng [1975], might explain other types of naturally occurring electromagnetic noise near the plasma frequency such as Type III radio noise bursts, $f > f_p$ noise, terrestrial kilometric radiation [Gurnett, 1974], etc.

These electrostatic noise bands are an excellent candidate for generating the $f > f_p$ electromagnetic noise (or non-thermal continuum radiation). Several cases are found for which the $f > f_p$ noise appears to be propagating away from regions containing intense electrostatic noise bands (see Figure 13 at 56.2 kHz, for example). In addition, the source region for the $f > f_p$ noise appears to be located on the dayside of the plasmasphere where essentially all of the twelve most intense cases of electrostatic noise bands were observed [see Gurnett, 1975].

A second possibility that may explain the wave magnetic field of these noise bands is that this noise is generated by a purely electrostatic instability, and that other electromagnetic modes are coupled to the electric field generated by particularly intense occurrences of the electrostatic noise. Some evidence to indicate this possibility

is found in the data collected by the University of Iowa experiment. Some examples are found that are more intense than those with an associated wave magnetic that have no wave magnetic field. In addition, there is no simple proportionality between the intensity of the wave electric field and that of the wave magnetic field (see Figures 15 and 16).

The observations of these electrostatic noise bands and the continuous transition between the upper hybrid resonance noise observed at lower altitudes in the plasmasphere, the electrostatic noise bands observed near the plasmapause, and the $(n + 1/2)f_g$ harmonics observed at larger radial distances in the outer magnetosphere strongly suggests that all these types of noise are related to the Harris electrostatic dispersion relation or to a corresponding electromagnetic dispersion relation that reduces to the electrostatic relation in the proper limit. It is suggested that instabilities generated by non-Maxwellian electron velocity distributions characteristic of the plasma sheet electron population generate these noise bands, similar to the theories proposed by Fredricks [1971] and Young et al. [1973] to explain the generation of the $(n + 1/2)f_g$ harmonics.

LIST OF REFERENCES

Allis, W. P., S. J. Buchsbaum, and A. Bers, Waves in Anisotropic Plasmas, MIT Press, Cambridge, Mass., 13, 1963.

Bauer, S. J., and R. G. Stone, Satellite observations of radio noise in the magnetosphere, Nature, 218, 1145, 1968.

Carpenter, D. L., C. G. Park, H. A. Taylor, Jr., and H. C. Brinton, Multi-experiment detection of the plasmapause from EOGO satellites and Antarctic ground stations, J. Geophys. Res., 74, 1837, 1969.

Chappell, C. R., K. K. Harris, and G. W. Sharp, The dayside of the plasmasphere, J. Geophys. Res., 76, 7632, 1971.

Cheng, C. Z., Ordinary electromagnetic mode instability, (in press), Journal of Plasma Physics, 1975.

DeForest, S. E., Spacecraft charging at synchronous orbit, J. Geophys. Res., 77, 651, 1972.

DeForest, S. E., and C. E. McIlwain, Plasma clouds in the magnetosphere, J. Geophys. Res., 76, 3587, 1971.

Dory, R. A., G. E. Guest, and E. G. Harris, Unstable electrostatic plasma waves propagating perpendicular to a magnetic field, Phys. Rev. Lett., 14, 131, 1965.

Frank, L. A., Relationship of the plasma sheet, ring current, trapping boundary, and plasmapause near the magnetic equator and local midnight, J. Geophys. Res., 76, 2265, 1971.

Fredricks, R. W., Plasma instability at $(n + 1/2)f_c$ and its relationship to some satellite observations, J. Geophys. Res., 76, 5344, 1971.

Fredricks, R. W., and F. L. Scarf, Recent studies of magnetospheric electric field emissions above the electron gyrofrequency, J. Geophys. Res., 78, 310, 1973.

Gregory, P. C., Radio emission from auroral electrons, Nature, 221, 350, 1969.

Gurnett, D. A., The earth as a radio source: terrestrial kilometric radiation, J. Geophys. Res., 79, 4227, 1974.

Gurnett, D. A., The earth as a radio source: the non-thermal continuum, (in press), J. Geophys. Res., 1975.

Gurnett, D. A., and L. A. Frank, Thermal and suprathermal plasma densities in the outer magnetosphere, J. Geophys. Res., 79, 2355, 1974.

Gurnett, D. A., and R. R. Shaw, Electromagnetic radiation trapped in the magnetosphere above the plasma frequency, J. Geophys. Res., 78, 8136, 1973.

Harris, E. G., Unstable plasma oscillations in a magnetic field, Phys. Rev. Lett., 2, 34, 1959.

Harris, K. K., G. W. Sharp, and C. R. Chappell, Observations of the plasmapause from OGO 5, J. Geophys. Res., 75, 219, 1970.

Hartz, T. R., Low frequency noise emissions and their significance for energetic particle processes in the polar ionosphere, The Polar Ionosphere and Magnetospheric Processes, Gordon Breach Publishing Co., New York, 151, 1970.

Kennel, C. F., F. L. Scarf, R. W. Fredricks, J. H. McGehee, and F. V. Coroniti, VLF electric field observations in the magnetosphere, J. Geophys. Res., 75, 6136, 1970.

Lyons, L. R., Electron diffusion driven by magnetospheric electrostatic waves, J. Geophys. Res., 79, 575, 1974.

Mosier, S. R., M. L. Kaiser, and L. W. Brown, Observations of noise bands associated with the upper hybrid resonance by the IMP-6 radio astronomy experiment, J. Geophys. Res., 78, 1673, 1973.

Muldrew, D. B., Preliminary results of ISIS 1 concerning electron density variations, ionospheric resonances, and Cerenkov radiation, Space Research X, North-Holland Publishing Co., Amsterdam, Holland, 786, 1970.

Russell, C. T., R. E. Holzer, and E. J. Smith, OGO 3 observations of ELF noise in the magnetosphere, 1. Spatial extend and frequency of occurrence, J. Geophys. Res., 74, 755, 1969.

Russell, C. T. and R. E. Holzer, AC magnetic fields, Particles and Fields in the Magnetosphere, D. Reidel Publishing Co., Dordrecht, Holland, 195, 1970.

Scarf, F. L., R. W. Fredricks, C. F. Kennel, and F. V. Coroniti, Satellite studies of magnetospheric substorms on August 15, 1968, J. Geophys. Res., 78, 3119, 1973.

Shaw, R. R. and D. A. Gurnett, Magnetospheric electron density measurements from upper hybrid resonance noise observed by IMP 6, U. of Iowa Research Report 72-37, 1972.

Stix, T. H., The Theory of Plasma Waves, McGraw-Hill, New York, 14, 1962.

Taylor, W. W. L., Generation and propagation of electromagnetic waves in the magnetosphere, U. of Iowa Research Report 73-16, 1973.

Taylor, W. W. L., and S. D. Shawhan, A test of incoherent Cerenkov radiation for VLF hiss and other magnetospheric emissions, J. Geophys. Res., 79, 105, 1974.

Thorne, R. M., E. J. Smith, R. K. Burton, and R. E. Holzer, Plasmaspheric hiss, J. Geophys. Res., 78, 1581, 1973.

Walsh, D., F. T. Haddock, and H. F. Schulte, Cosmic radio intensities at 1.225 and 2.0 Mc measured up to an altitude of 1700 km, Space Research IV, North-Holland Publishing Co., Amsterdam, Holland, 935, 1964.

Young, T. S. T., J. D. Callen, and J. E. McCune, High frequency electrostatic waves in the magnetosphere, J. Geophys. Res., 78, 1082, 1973.

APPENDIX: FIGURES

Figure 1 The projection of a typical IMP 6 orbit on the ecliptic plane. The spacecraft samples all local times equally in approximately one year. It spends about ten percent of the time at radial distances below ten earth radii inside the magnetosphere, and it samples a path from inside the plasmasphere to the magnetopause in about five hours.

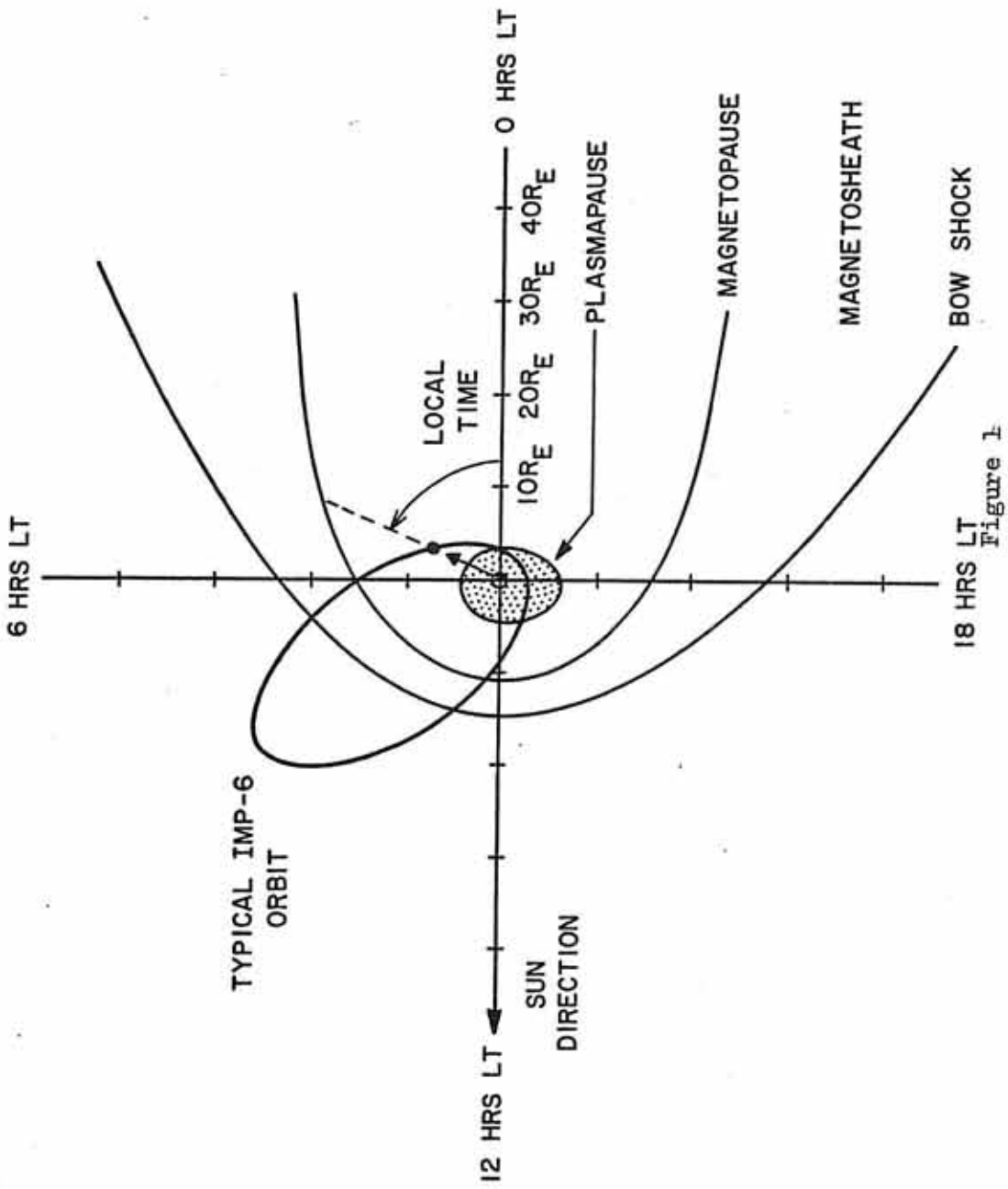
A-675-1
0 HRS LT
6 HRS LT
18 HRS LT
12 HRS LT
10RE
20RE
30RE
40RE
LOCAL TIME
PLASMAPAUSE
MAGNETOPAUSE
MAGNETOSHEATH
BOW SHOCK
TYPICAL IMP-6 ORBIT
SUN DIRECTION

Figure 1

Figure 2 A drawing of the IMP 6 spacecraft illustrating the complement of seven antennas used by the University of Iowa plasma wave experiment. Three mutually orthogonal "long-wire" dipole antennas and a "short electric" antenna are used to detect wave electric fields. Three mutually orthogonal magnetic loop antennas are used to detect wave magnetic fields.

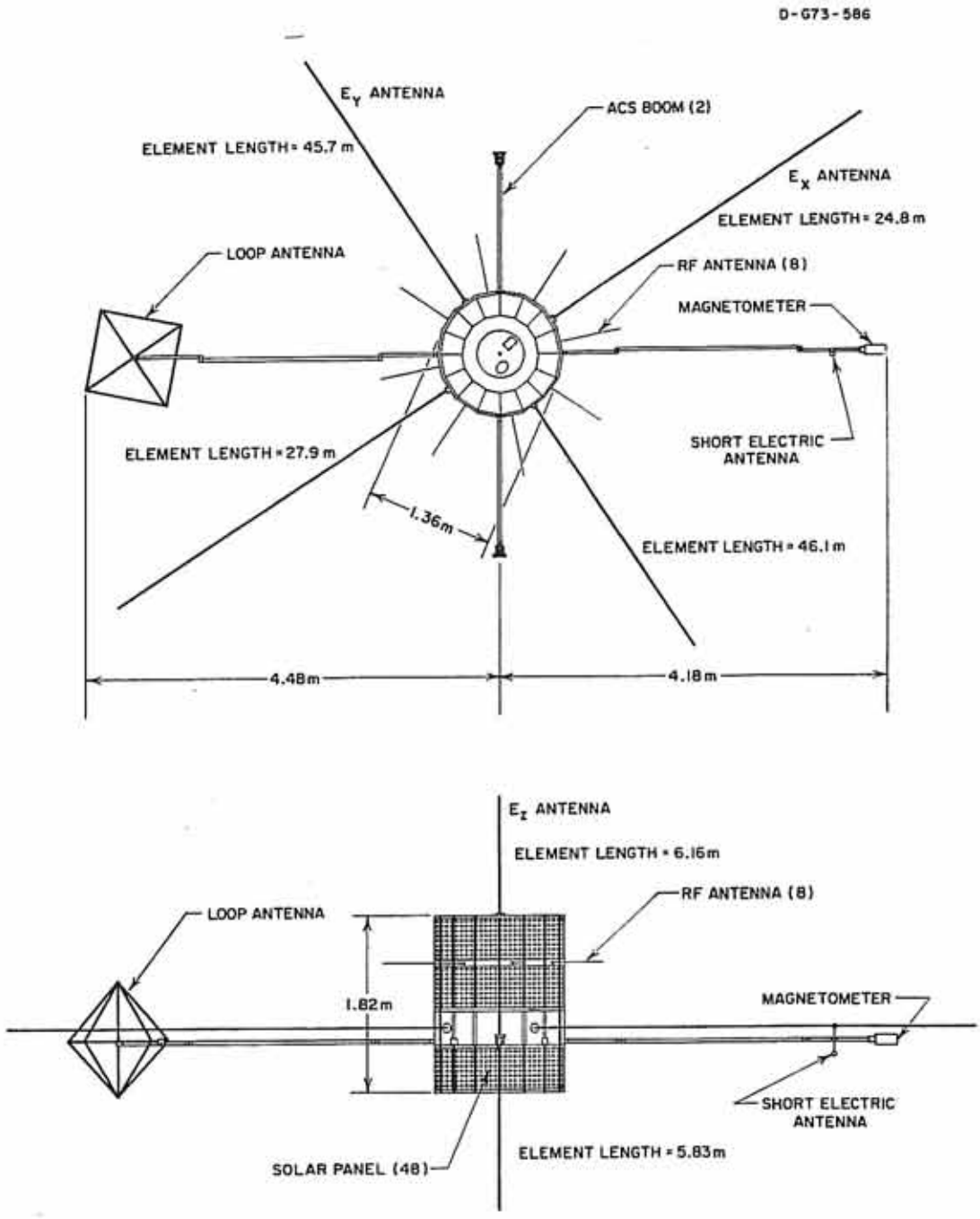
D-G73-586
E_Y ANTENNA
ELEMENT LENGTH = 45.7 m
ACS BOOM (2)
E_X ANTENNA
ELEMENT LENGTH = 24.8 m
LOOP ANTENNA
RF ANTENNA (8)
MAGNETOMETER
SHORT ELECTRIC ANTENNA
ELEMENT LENGTH = 27.9 m
1.36m
ELEMENT LENGTH = 46.1 m
4.48m
4.18m
E_Z ANTENNA
ELEMENT LENGTH = 6.16m
RF ANTENNA (8)
LOOP ANTENNA
1.82m
MAGNETOMETER
SHORT ELECTRIC ANTENNA
SOLAR PANEL (48)
ELEMENT LENGTH = 5.83m

Figure 2

Figure 3 A block diagram of the two digital spectrum analyzers, which perform in-flight frequency spectrum analysis, and the associated antenna switching circuitry. Any pair of the seven antennas may be connected to the spectrum analyzers by ground commands. Each spectrum analyzer has sixteen filter channels covering the frequency range from 20 Hz to 200 kHz. Each filter channel has a dynamic range of 100 db and has two detectors, a peak detector and an average detector. The peak detector measures the largest signal strength seen in a 5.11 second sample interval, and the average detector measures a time average signal strength over a 5.11 second interval. The spectrum analyzers used in conjunction with the long electric antennas measure wave electric field strengths as low as 0.2 microvolts per meter.

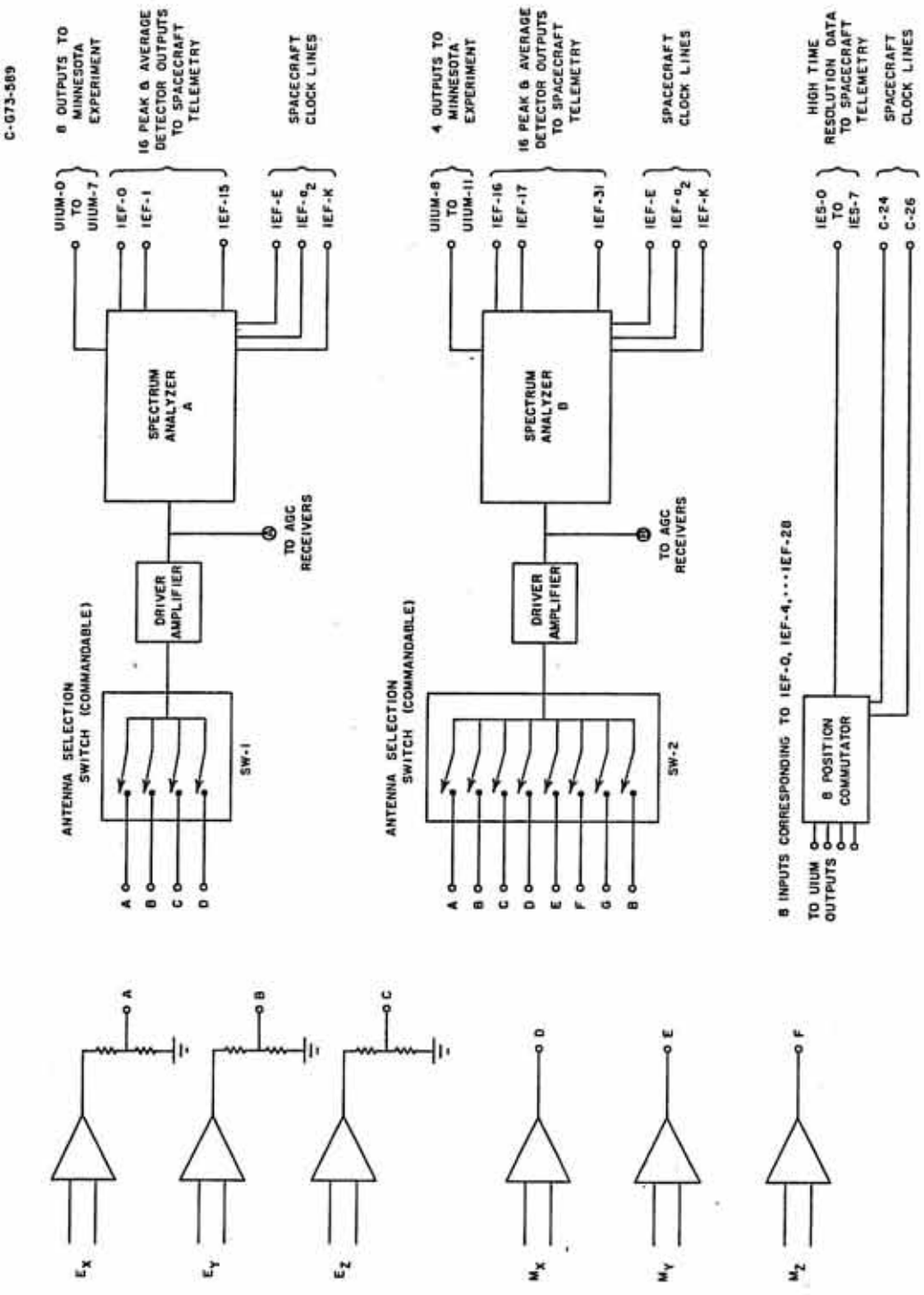
C-673-589
8 OUTPUTS TO MINNESOTA EXPERIMENT
16 PEAK & AVERAGE DETECTOR OUTPUTS TO SPACECRAFT TELEMETRY
SPACECRAFT CLOCK LINES
UIUM-0 TO UIUM-7
IEF-0
IEF-1
IEF-15
IEF-E
IEF-σ_2
IEF-K
SPECTRUM ANALYZER A
TO AGC RECEIVERS
DRIVER AMPLIFIER
ANTENNA SELECTION SWITCH (COMMANDABLE)
SW-1
A
B
C
D
4 OUTPUTS TO MINNESOTA EXPERIMENT
UIUM-8 TO UIUM-11
IEF-16
IEF-17
IEF-31
SPECTRUM ANALYZER B
SW-2
E
F
G
H
HIGH TIME RESOLUTION DATA TO SPACECRAFT TELEMETRY
IES-0 TO IES-7
C-24
C-26
8 INPUTS CORRESPONDING TO IEF-0, IEF-4, ··· IEF-28
8 POSITION COMMUTATOR
TO UIUM OUTPUTS
E_X
E_Y
E_Z
M_X
M_Y
M_Z
SE

Figure 3

Figure 4 A block diagram of the two AGC receivers used for the analysis of narrow band and transient wave phenomena. Eight commandable modes of operation provide for a variety of operating configurations that include modes controlled by the spacecraft clock lines. Data researched for this report were usually recorded in the mode in which AGC receiver no. 1 cycles between the electric and magnetic antennas and the frequency ranges 650 Hz - 10 kHz, 11 kHz - 19 kHz, and 21 kHz - 29 kHz. Additional frequency coverage below 1 kHz is provided by AGC receiver no. 2 which also cycles between the electric and magnetic antennas.

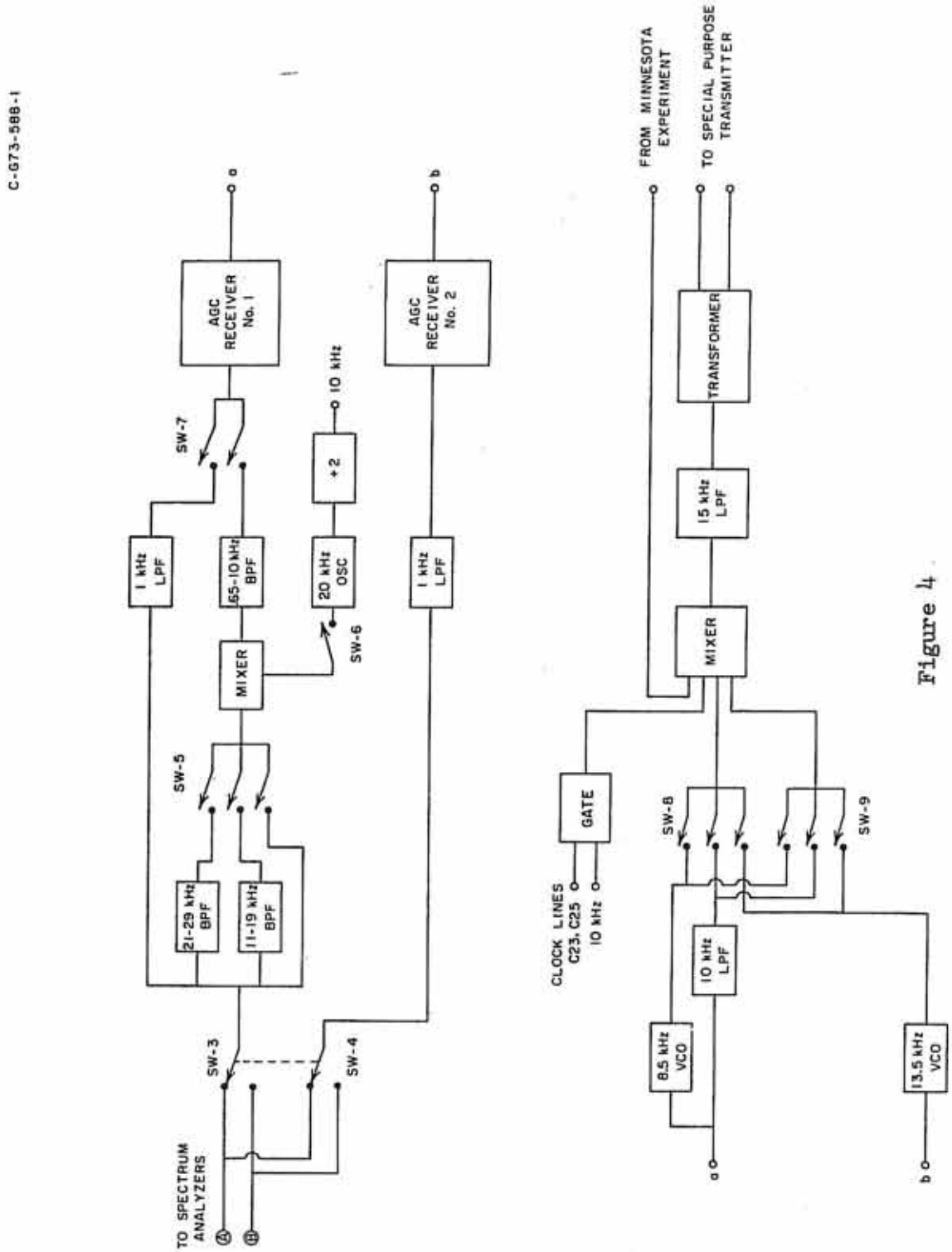
C-G73-588-1
a
AGC RECEIVER No. 1
SW-7
1 kHz LPF
65-110 kHz BPF
MIXER
SW-5
21-29 kHz BPF
11-19 kHz BPF
SW-3
SW-4
TO SPECTRUM ANALYZERS
A
B
10 kHz
+2
20 kHz OSC
SW-6
b
AGC RECEIVER No. 2
1 kHz LPF
FROM MINNESOTA EXPERIMENT
TO SPECIAL PURPOSE TRANSMITTER
TRANSFORMER
15 kHz LPF
MIXER
GATE
CLOCK LINES C23, C25 10 kHz
SW-8
SW-9
10 kHz LPF
8.5 kHz VCO
13.5 kHz VCO
a
b

Figure 4

Figure 5 Spectrum analyzer data from a typical outbound IMP 6 magnetospheric pass from near 2.0 earth radii to 10.0 earth radii geocentric radial distance. The inset shows an electrostatic noise band of the type found on about two-thirds of all IMP 6 passes through this region of the magnetosphere. The noise band decreases in frequency with increasing radial distance with an abrupt decrease in frequency near the plasmapause. The plasmapause is identified by the sudden increase in the magnitude of the solar array interference in the low frequency electric antenna channels and by the sudden termination of the plasmaspheric hiss in the low frequency magnetic antenna channels. The frequency of the bands both inside and just outside the plasmapause is near the local plasma frequency typically observed in these respective regions.

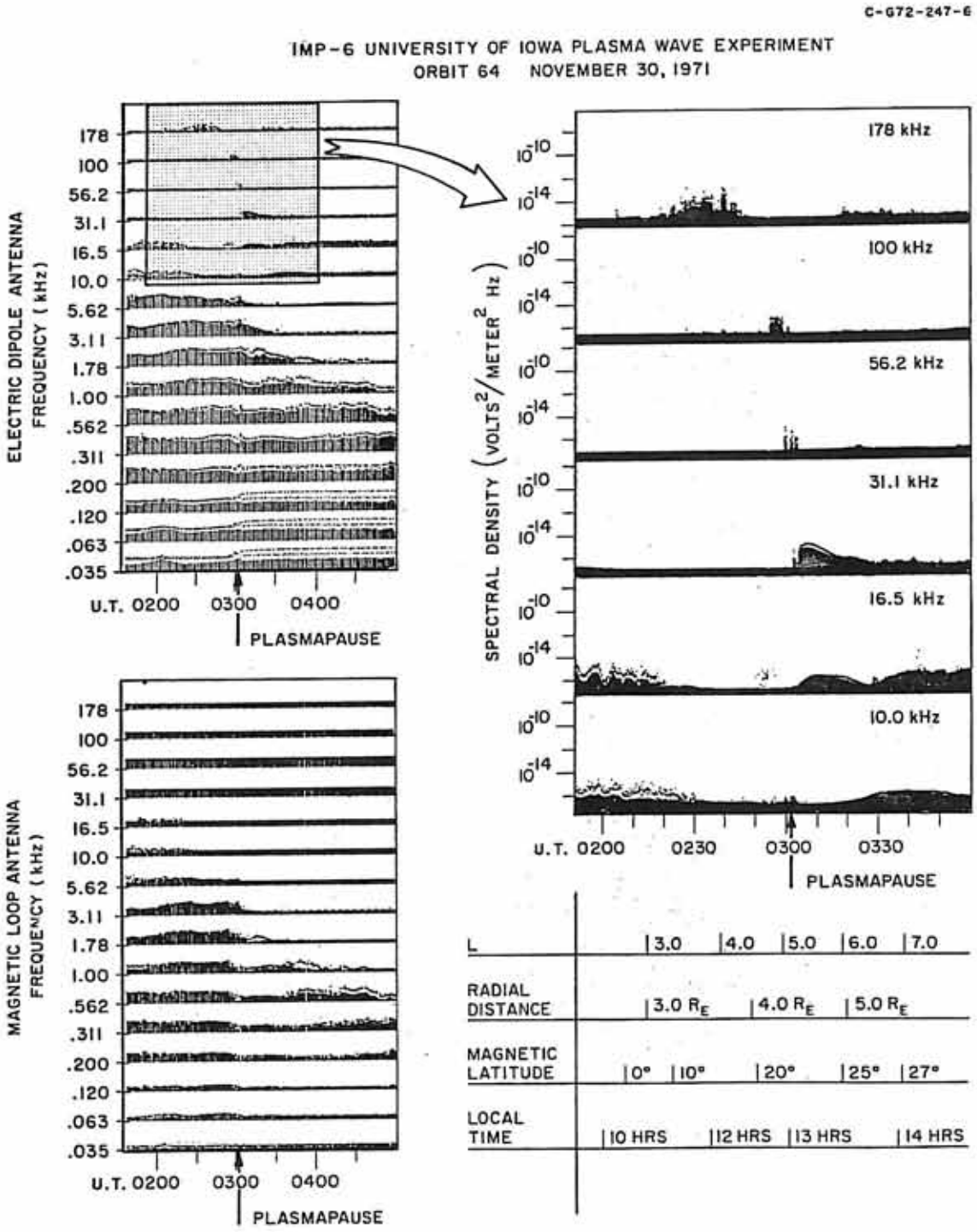
C-G72-247-6
IMP-6 UNIVERSITY OF IOWA PLASMA WAVE EXPERIMENT
ORBIT 64 NOVEMBER 30, 1971
ELECTRIC DIPOLE ANTENNA FREQUENCY (kHz)
178
100
56.2
31.1
16.5
10.0
5.62
3.11
1.78
1.00
.562
.311
.200
.120
.063
.035
U.T. 0200
0300
0400
PLASMAPAUSE
MAGNETIC LOOP ANTENNA FREQUENCY (kHz)
SPECTRAL DENSITY (VOLTS²/METER² Hz)
178 kHz
100 kHz
56.2 kHz
31.1 kHz
16.5 kHz
10.0 kHz
10⁻¹⁰
10⁻¹⁴
U.T. 0200
0230
0300
0330
PLASMAPAUSE
L
3.0
4.0
5.0
6.0
7.0
RADIAL DISTANCE
3.0 R_E
4.0 R_E
5.0 R_E
MAGNETIC LATITUDE
0°
10°
20°
25°
27°
LOCAL TIME
10 HRS
12 HRS
13 HRS
14 HRS

Figure 5

Figure 6 The location of the largest signal strength seen in the 31.1 kHz filter channel for all electrostatic noise bands of the type shown in Figure 5. The data surveyed were the result of a full year of operation of the University of Iowa IMP 6 plasma wave experiment; therefore, all local times were nearly evenly sampled. The bands are found at all local times, occurring least frequently from 18 to 24 hours. At 31.1 kHz they occur at radial distances near four to five earth radii and tend to occur at somewhat larger radial distances near local evening than near local morning. This corresponds roughly with the average location of the plasmapause as would be expected if the bands occur at frequencies near the local plasma frequency.

A-G73-625-1

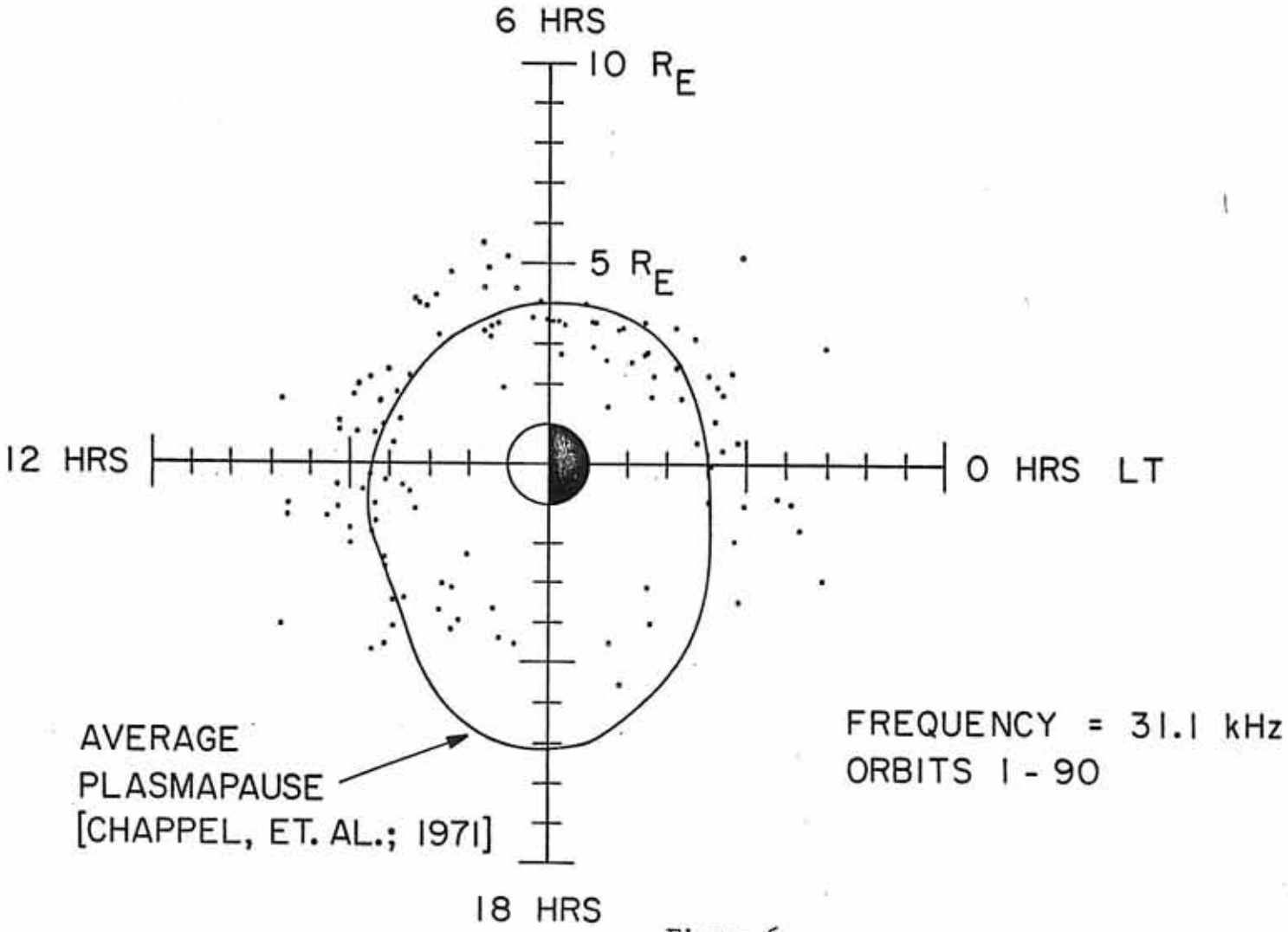

Figure 6

Figure 7 An inbound IMP 6 magnetospheric pass, orbit 18, from about eleven earth radii to two earth radii geocentric radial distance illustrating an example of narrow band electrostatic noise. The narrow band electrostatic noise is resolved into four distinct bands in the wideband receiver data that occur at frequencies between consecutive harmonics of the electron gyrofrequency as determined by measurements from the NASA/GSFC magnetometer experiment. The bands tend to occur between higher harmonic numbers as the spacecraft moves to larger radial distances beyond the plasmapause. This behavior, the abrupt change in frequency in crossing the plasmapause, and the identification of the plasma frequency at 0620 UT, all suggest that the local plasma frequency has a strong influence on the frequency at which the narrow band electrostatic noise occurs.

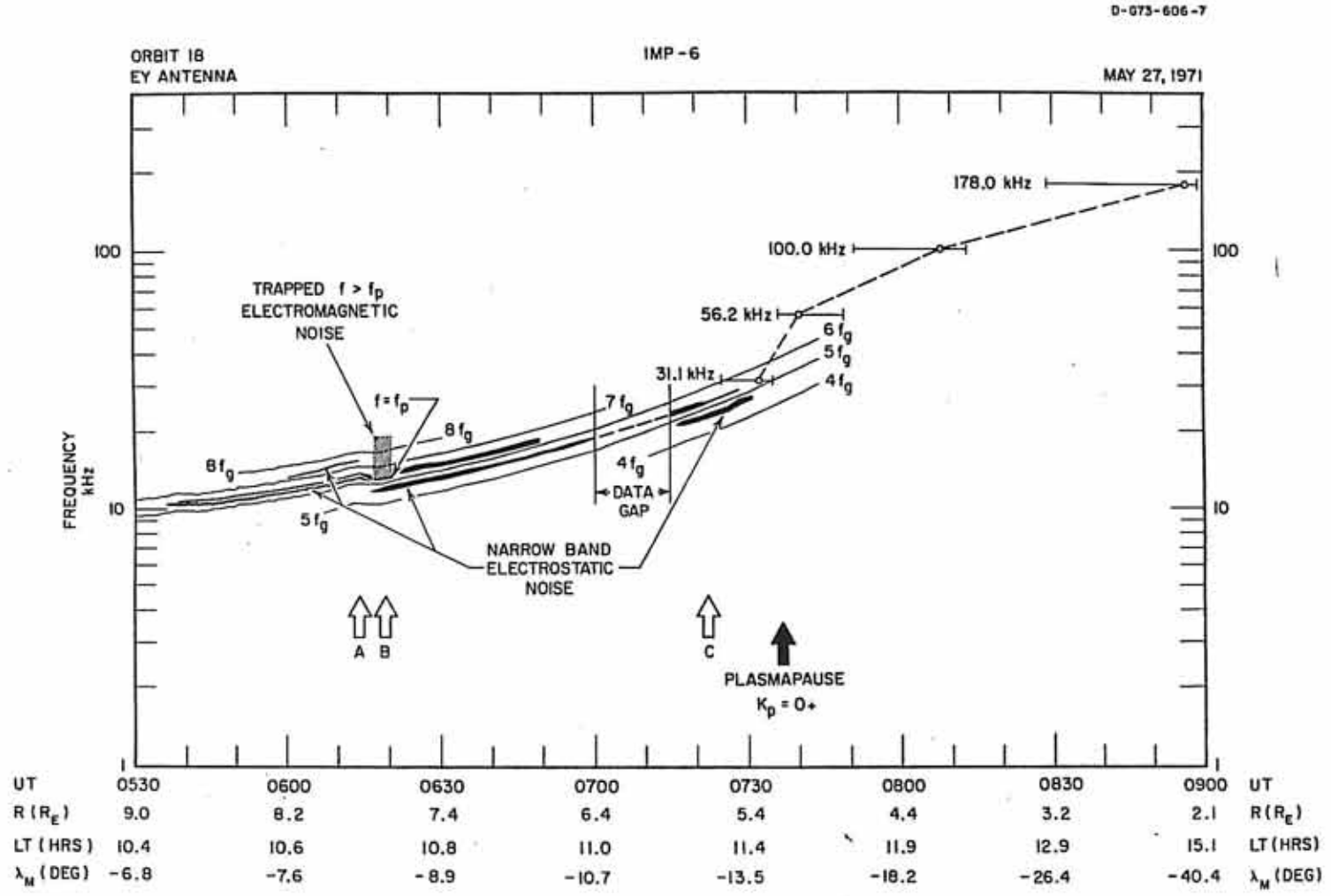
D-073-606-7
ORBIT 18
EY ANTENNA
IMP-6
MAY 27, 1971
178.0 kHz
100.0 kHz
56.2 kHz
31.1 kHz
100
10
FREQUENCY kHz
TRAPPED f > fp ELECTROMAGNETIC NOISE
f = fp
8 fg
7 fg
6 fg
5 fg
4 fg
DATA GAP
NARROW BAND ELECTROSTATIC NOISE
A
B
C
PLASMAPAUSE
Kp = 0+
UT 0530 0600 0630 0700 0730 0800 0830 0900 UT
R (RE) 9.0 8.2 7.4 6.4 5.4 4.4 3.2 2.1 R (RE)
LT (HRS) 10.4 10.6 10.8 11.0 11.4 11.9 12.9 15.1 LT (HRS)
λM (DEG) -6.8 -7.6 -8.9 -10.7 -13.5 -18.2 -26.4 -40.4 λM (DEG)

Figure 7

Figure 8 Wideband spectrograms of the narrow band electrostatic noise at points labeled A, B, and C in Figure 7. The narrow band electrostatic noise consists of several well defined lines, which do not have nulls in intensity as the spacecraft rotates as does the trapped $f > f_p$ electromagnetic noise observed at 0620 UT in spectrogram B. The absence of spin-modulated intensity suggests that the direction of the wave electric field vector of the narrow band electrostatic noise is not strongly oriented parallel or perpendicular to the geomagnetic field.

C-G73-609-1

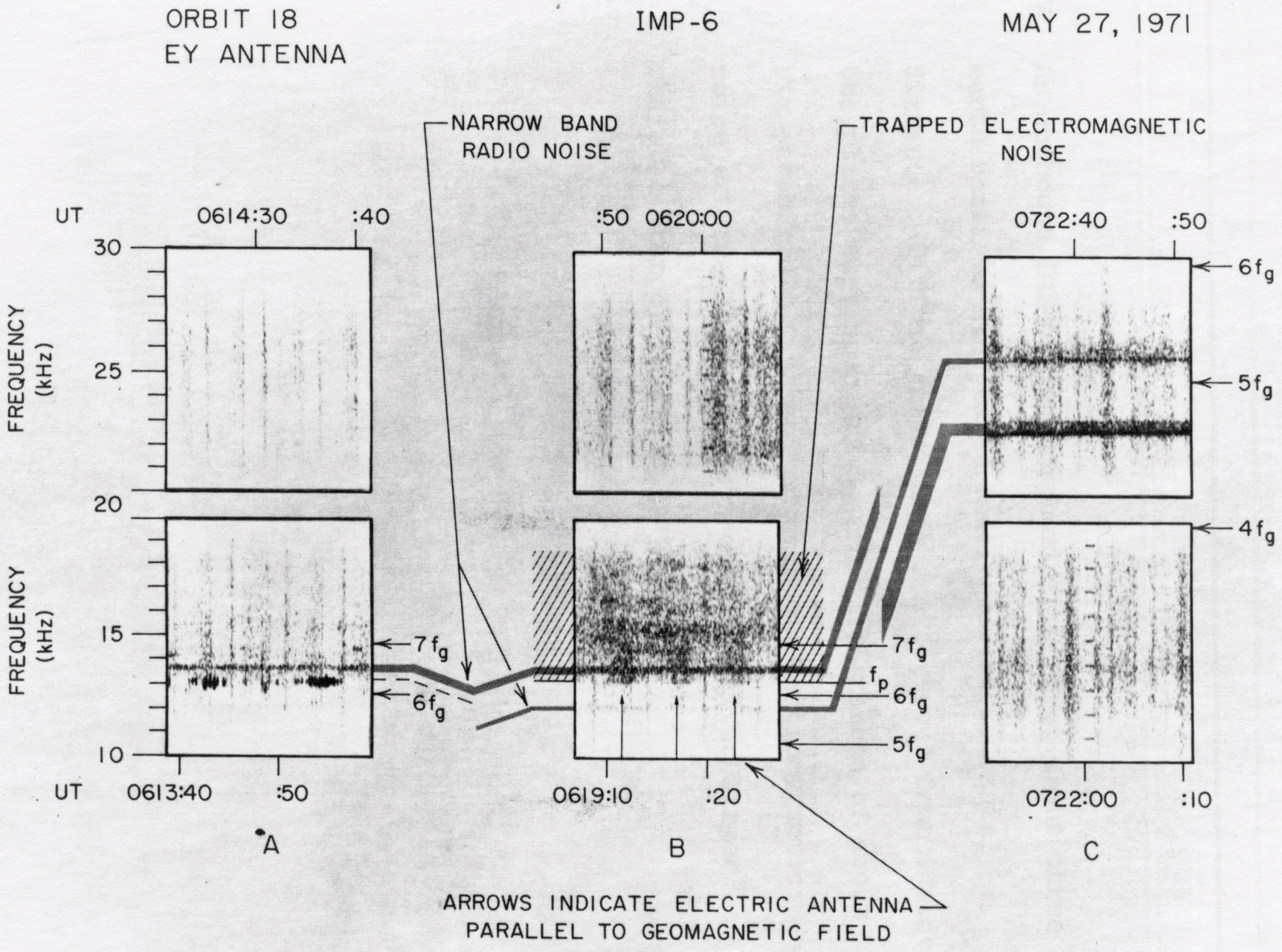
ORBIT 18
EY ANTENNA
IMP-6
MAY 27, 1971
NARROW BAND RADIO NOISE
TRAPPED ELECTROMAGNETIC NOISE
UT
0614:30
:40
:50
0620:00
0722:40
:50
FREQUENCY (kHz)
30
25
20
15
10
6fg
5fg
4fg
7fg
6fg
fp
6fg
5fg
UT
0613:40
:50
0619:10
:20
0722:00
:10
A
B
C
ARROWS INDICATE ELECTRIC ANTENNA PARALLEL TO GEOMAGNETIC FIELD

Figure 9 An outbound IMP 6 magnetospheric pass, orbit 78, from about three earth radii to eight earth radii geocentric radial distance illustrating an example of diffuse electrostatic noise. The diffuse electrostatic noise is resolved into three distinct bands in the wideband receiver data. These noise bands are bounded by consecutive harmonics of the electron gyrofrequency determined by measurements from the NASA/GSFC magnetometer experiment as indicated. The noise bands tend to occur between harmonics that are near the local plasma frequency as identified from the lower cutoff frequency of the trapped $f > f_p$ electromagnetic noise.

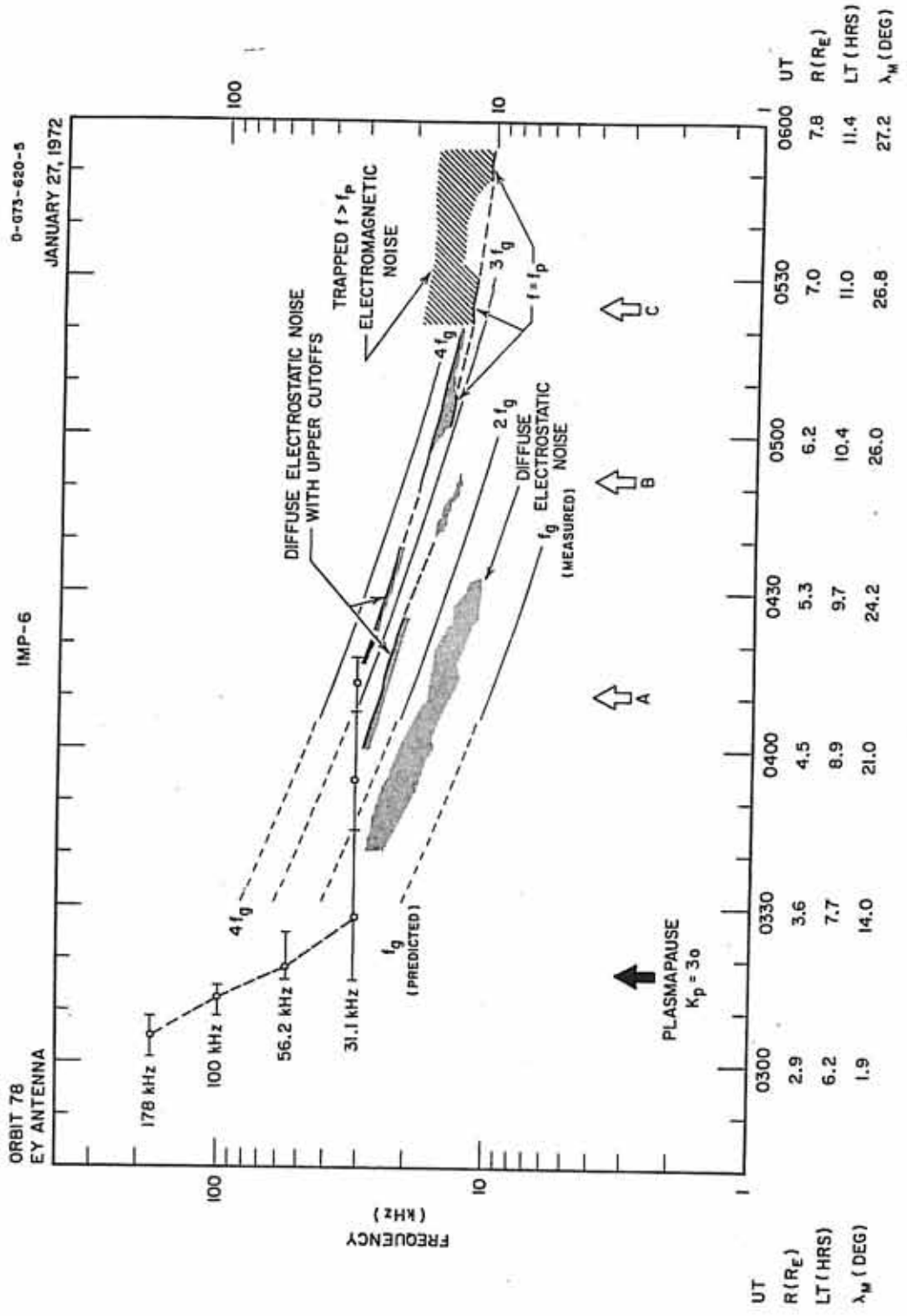
IMP-6
JANUARY 27, 1972
D-073-620-5
ORBIT 78
EY ANTENNA
FREQUENCY (kHz)
100
10
1
178 kHz
100 kHz
56.2 kHz
31.1 kHz
$4f_g$
f_g (PREDICTED)
DIFFUSE ELECTROSTATIC NOISE WITH UPPER CUTOFFS
TRAPPED $f > f_p$ ELECTROMAGNETIC NOISE
$4f_g$
$3f_g$
$f = f_p$
$2f_g$
DIFFUSE f_g ELECTROSTATIC NOISE (MEASURED)
PLASMAPAUSE $K_p = 3o$
A
B
C
UT 0300 0330 0400 0430 0500 0530 0600
R(R_E) 2.9 3.6 4.5 5.3 6.2 7.0 7.8
LT (HRS) 6.2 7.7 8.9 9.7 10.4 11.0 11.4
λ_M (DEG) 1.9 14.0 21.0 24.2 26.0 26.8 27.2
UT
R(R_E)
LT (HRS)
λ_M (DEG)

Figure 9

Figure 10 Wideband spectrograms of the diffuse electrostatic noise at points labeled A, B, and C in Figure 9. The diffuse electrostatic noise consists of faint noise, several kHz in width, sometimes with a sharp upper cutoff frequency. The diffuse noise bands frequently have nulls that occur at twice the spacecraft spin rate. The position of these nulls indicates that the electric field vector of the noise bands is oriented perpendicular to the geomagnetic field. A lower cutoff frequency which appears to be at the local plasma frequency develops for a short time near 0505 UT.

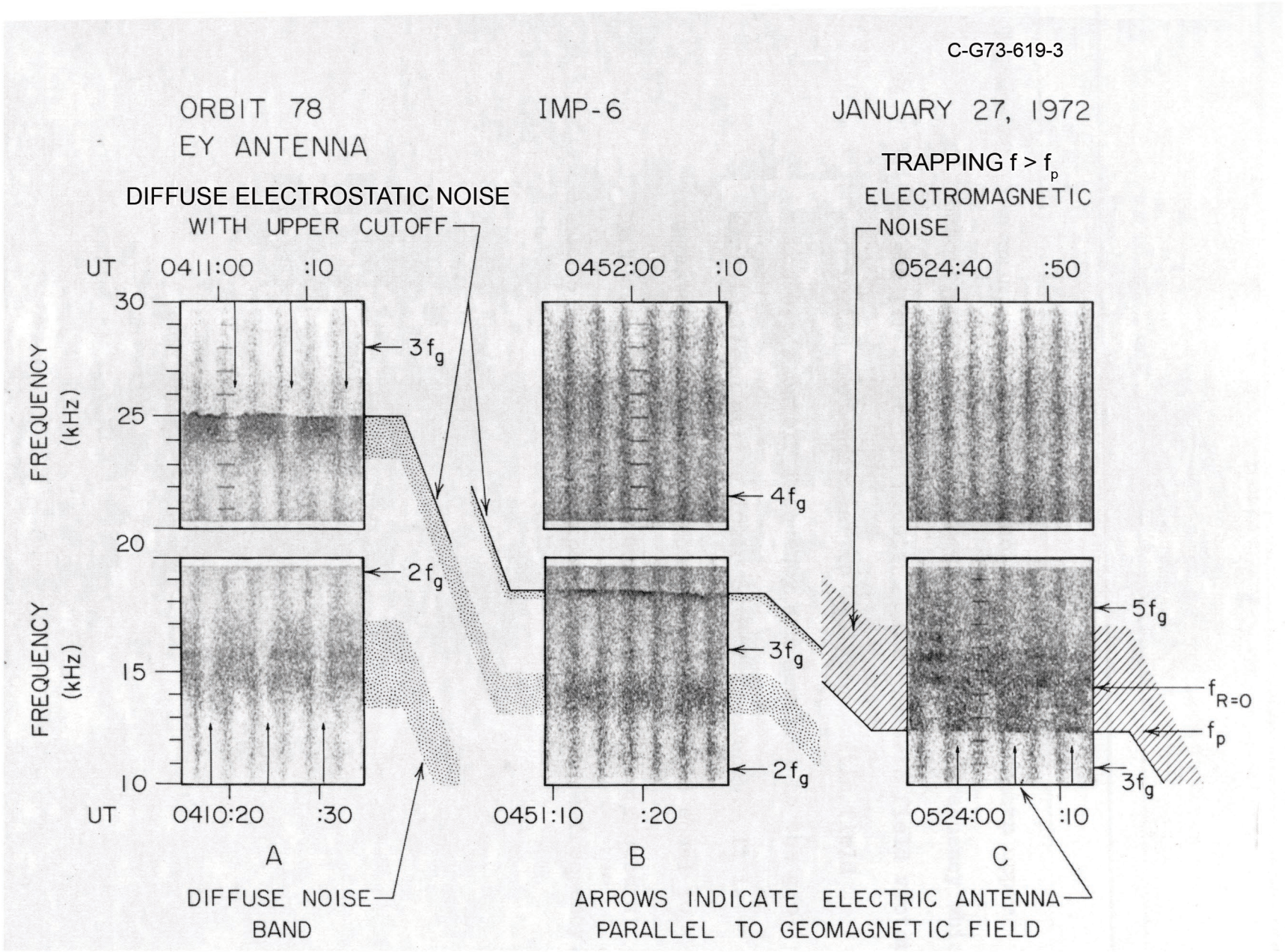
C-G73-619-3
ORBIT 78
EY ANTENNA
IMP-6
JANUARY 27, 1972
TRAPPING f > f_p
ELECTROMAGNETIC
NOISE
DIFFUSE ELECTROSTATIC NOISE
WITH UPPER CUTOFF
UT 0411:00 :10
0452:00 :10
0524:40 :50
FREQUENCY (kHz)
30
25
20
15
10
$3f_g$
$4f_g$
$2f_g$
$5f_g$
$f_{R=0}$
f_p
UT 0410:20 :30
0451:10 :20
0524:00 :10
A
B
C
DIFFUSE NOISE BAND
ARROWS INDICATE ELECTRIC ANTENNA PARALLEL TO GEOMAGNETIC FIELD

Figure 11 The frequency of occurrence of the peak electric field spectral density of the noise bands at 31.1 kHz. The occurrence in percent is based on the total number of magnetospheric passes in the first year of operation of the University of Iowa IMP 6 plasma wave experiment. These noise bands occurred on about two-thirds of all magnetospheric passes with a peak electric field spectral density most often near 10^{-15} volts^2 meter^{-2} Hz^{-1}. This is equivalent to a broadband field strength of about two microvolts per meter.

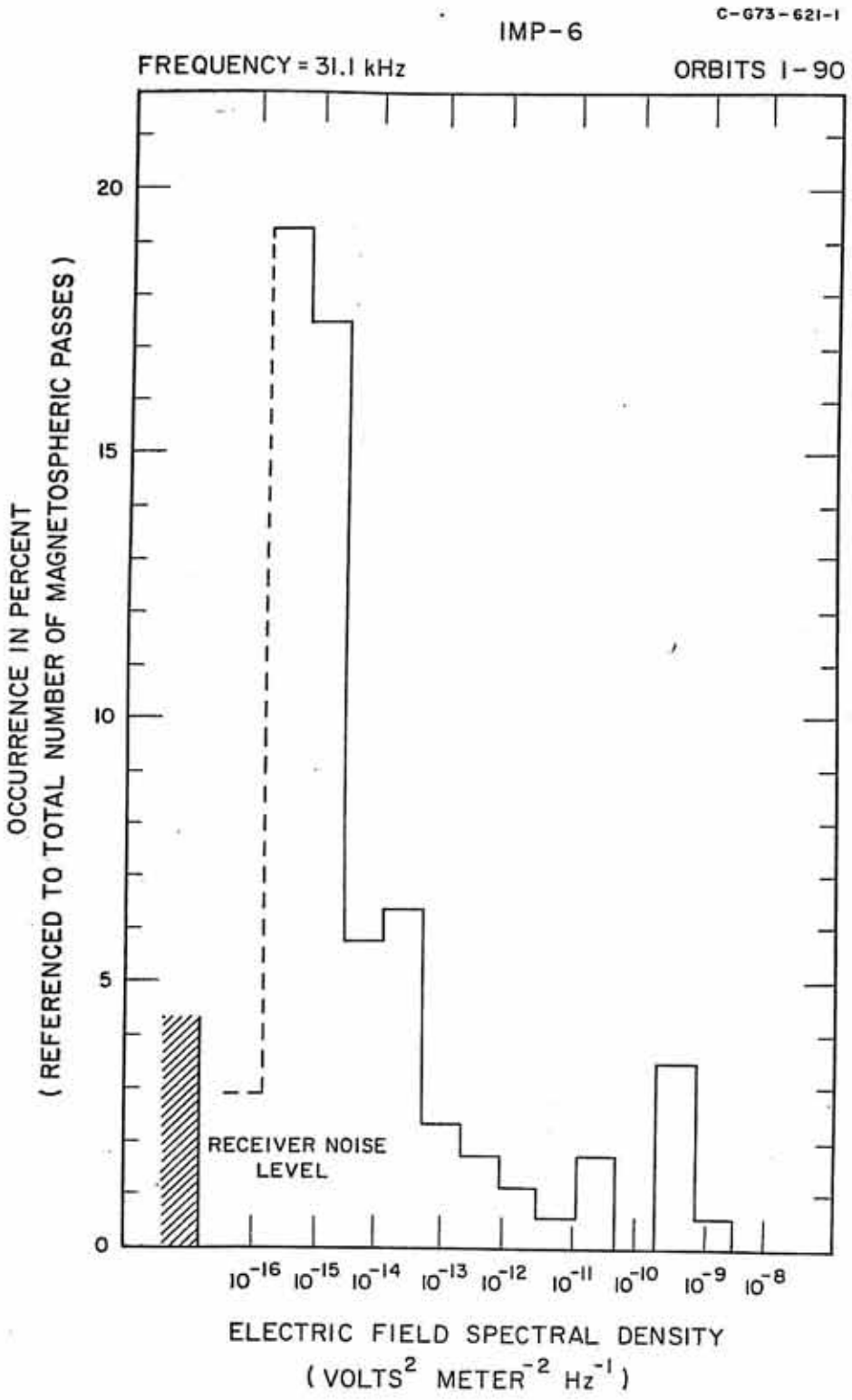
C-G73-621-1
IMP-6
FREQUENCY = 31.1 kHz
ORBITS 1-90
OCCURRENCE IN PERCENT
(REFERENCED TO TOTAL NUMBER OF MAGNETOSPHERIC PASSES)
20
15
10
5
0
RECEIVER NOISE
LEVEL
10^{-16} 10^{-15} 10^{-14} 10^{-13} 10^{-12} 10^{-11} 10^{-10} 10^{-9} 10^{-8}
ELECTRIC FIELD SPECTRAL DENSITY
(VOLTS^2 METER^{-2} Hz^{-1})

Figure 11

Figure 12 The peak electric field spectral density as a function of the peak magnetic field spectral density for the eight out of 110 cases in which noise bands were observed with a wave magnetic field component. The value of the wave magnetic field energy density is about four orders of magnitude less than the value of the electric field energy density, and these eight cases correspond to observations for which the bands have unusually intense electric field strengths. Five other cases exist with wave electric field spectral densities between 10^{-11} volts^2 meter^{-2} Hz^{-1} and 10^{-8} volts^2 meter^{-2} Hz^{-1} for which no wave magnetic field was detected.

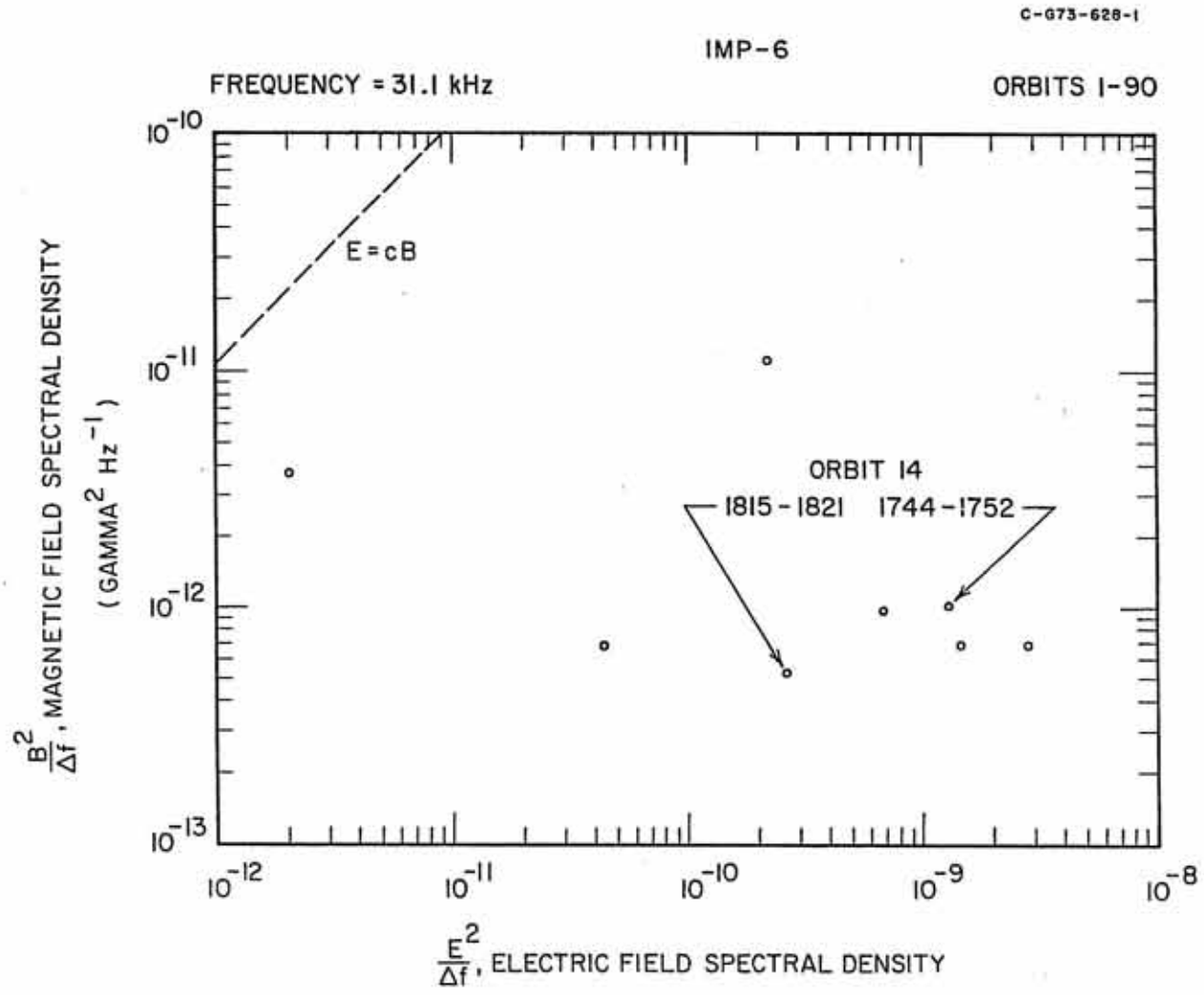
C-G73-628-1
IMP-6
FREQUENCY = 31.1 kHz
ORBITS 1-90
E=cB
ORBIT 14
1815-1821
1744-1752
10^{-10}
10^{-11}
10^{-12}
10^{-13}
10^{-12}
10^{-11}
10^{-10}
10^{-9}
10^{-8}
$\frac{B^2}{\Delta f}$, MAGNETIC FIELD SPECTRAL DENSITY
(GAMMA^2 Hz^{-1})
$\frac{E^2}{\Delta f}$, ELECTRIC FIELD SPECTRAL DENSITY
(VOLTS^2 METER^{-2} Hz^{-1})

Figure 12

Figure 13 The raw voltage outputs of the highest six spectrum analyzer filter channels for an inbound magnetospheric pass that contains unusually intense noise bands at 31.1 kHz near the plasmapause at three earth radii. These noise bands are observed to have a wave magnetic field coincidently with the large amplitude electric field.

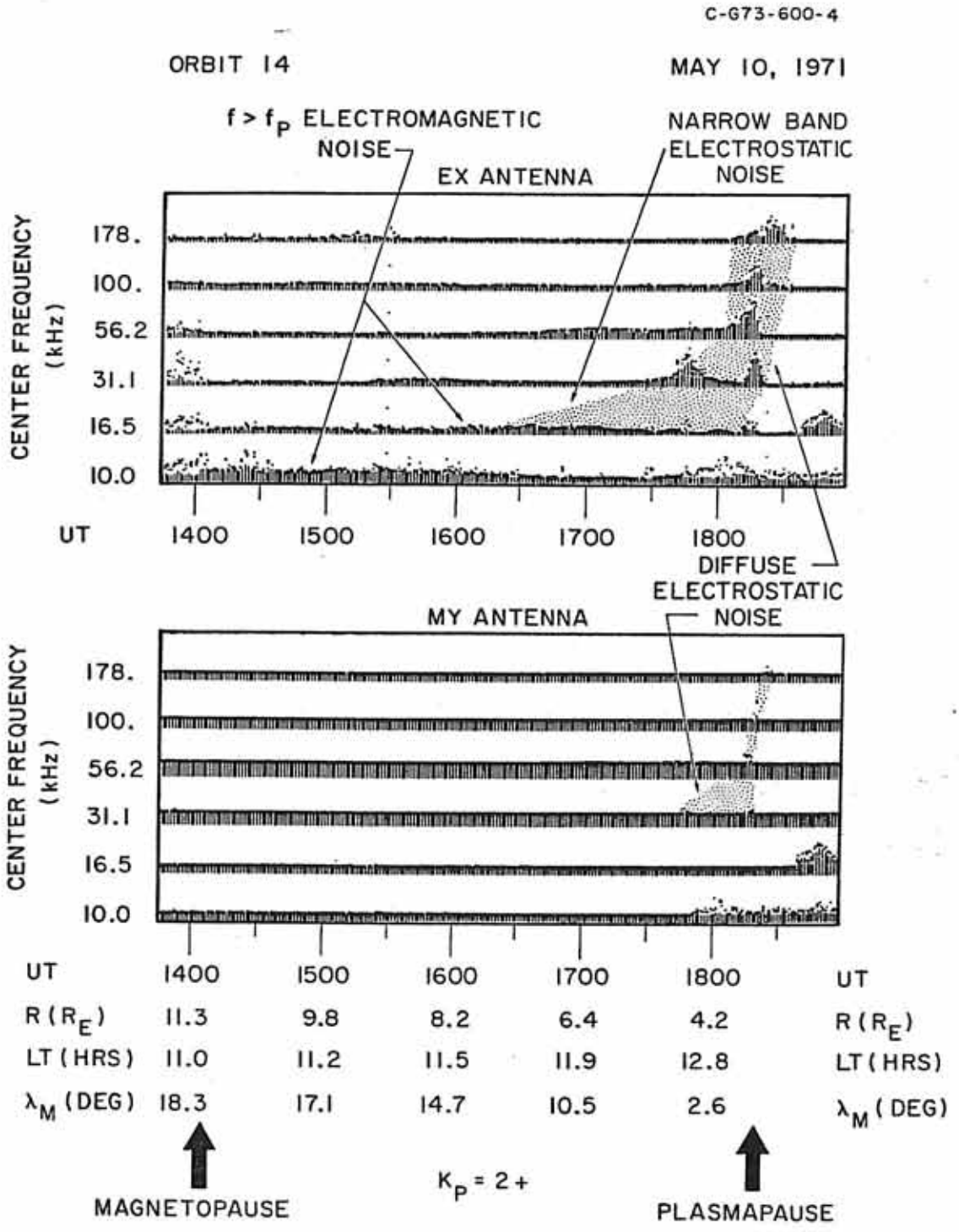
C-G73-600-4
ORBIT 14
MAY 10, 1971
f > f_P ELECTROMAGNETIC NOISE
NARROW BAND ELECTROSTATIC NOISE
EX ANTENNA
CENTER FREQUENCY (kHz)
178.
100.
56.2
31.1
16.5
10.0
UT
1400
1500
1600
1700
1800
DIFFUSE ELECTROSTATIC NOISE
MY ANTENNA
CENTER FREQUENCY (kHz)
178.
100.
56.2
31.1
16.5
10.0
UT 1400 1500 1600 1700 1800 UT
R (R_E) 11.3 9.8 8.2 6.4 4.2 R (R_E)
LT (HRS) 11.0 11.2 11.5 11.9 12.8 LT (HRS)
λ_M (DEG) 18.3 17.1 14.7 10.5 2.6 λ_M (DEG)
MAGNETOPAUSE
K_P = 2+
PLASMAPAUSE

Figure 13

Figure 14 The high resolution wideband receiver data from the E_x antenna resolve the intense noise bands shown in Figure 13 into five distinct bands. The spectral characteristics of the three bands in the intervals f_g to $2f_g$, $2f_g$ to $3f_g$, and $3f_g$ to $4f_g$ are similar to those of the diffuse electrostatic noise. The two bands in the intervals $4f_g$ to $5f_g$ and $5f_g$ to $6f_g$ are characteristic of the narrow band electrostatic noise. No signals were observed in the magnetic antenna wideband receiver data; therefore, it is not possible to determine if the wave magnetic field is associated with only one spectral type of noise or with both types.

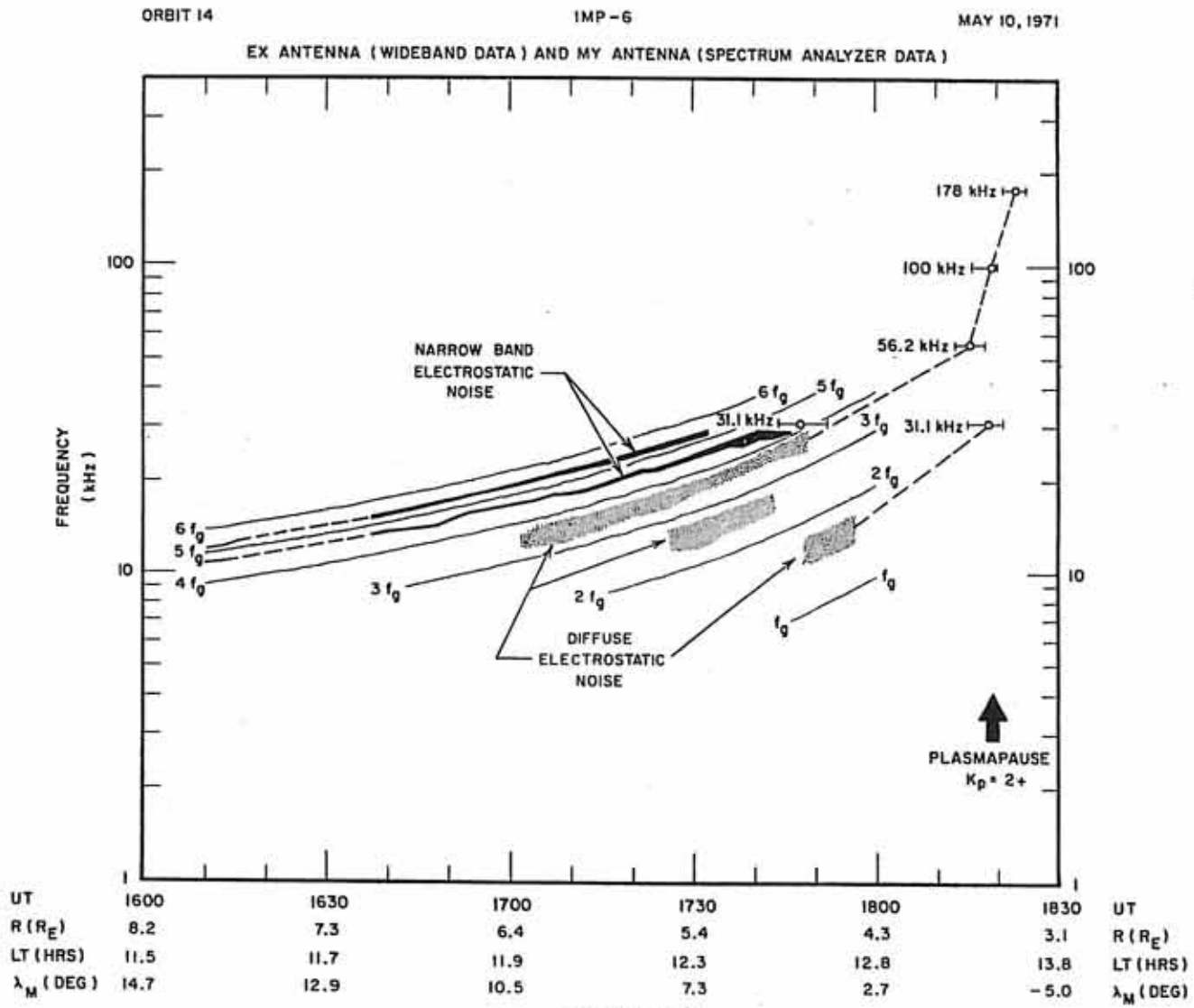
ORBIT 14
IMP-6
MAY 10, 1971
EX ANTENNA (WIDEBAND DATA) AND MY ANTENNA (SPECTRUM ANALYZER DATA)
FREQUENCY (kHz)
100
10
1
178 kHz
100 kHz
56.2 kHz
31.1 kHz
31.1 kHz
NARROW BAND ELECTROSTATIC NOISE
6 f_g
5 f_g
4 f_g
3 f_g
2 f_g
f_g
DIFFUSE ELECTROSTATIC NOISE
PLASMAPAUSE
K_p = 2+
UT 1600 1630 1700 1730 1800 1830 UT
R (R_E) 8.2 7.3 6.4 5.4 4.3 3.1 R (R_E)
LT (HRS) 11.5 11.7 11.9 12.3 12.8 13.8 LT (HRS)
λ_M (DEG) 14.7 12.9 10.5 7.3 2.7 -5.0 λ_M (DEG)

Figure 14

Figure 15 A plot of the wave magnetic field spectral density as a function of the wave electric field spectral density for the noise bands on the inbound pass of orbit 14. The data plotted are the outputs of the peak detector of the 31.1 kHz filter channel, which is sampled once each 5.11 seconds. The noise level spectral density of the magnetic receiver has been subtracted from the received signal to reduce the error caused by noise at small signal levels. The magnetic field energy density of the bands is one to four orders of magnitude less than the electric field energy density. The wave magnetic field of the noise bands tends to increase as the electric field increases; however, for a particular value of magnetic field spectral density the electric field spectral density varies by about three orders of magnitude.

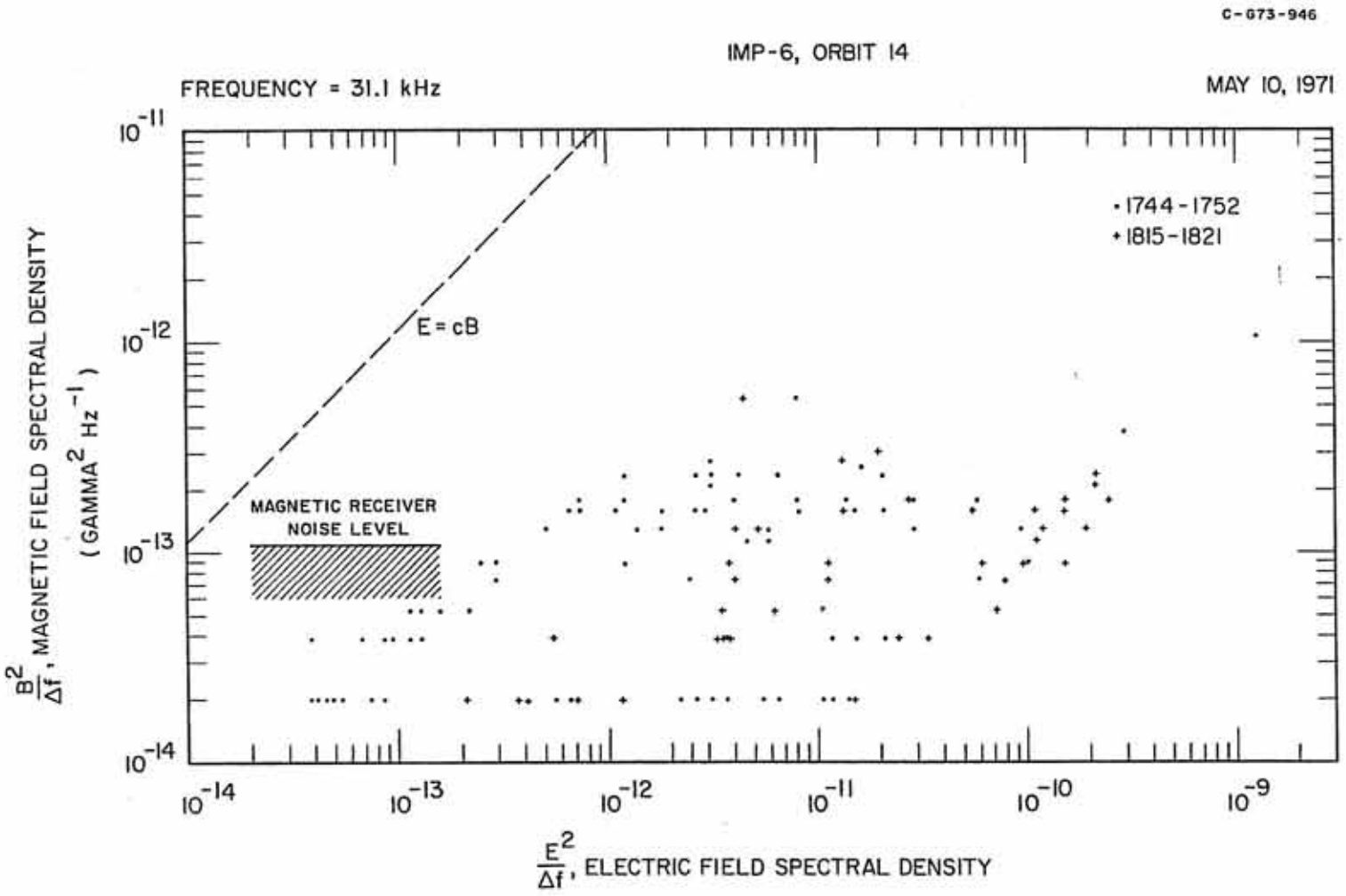
C-673-946
IMP-6, ORBIT 14
FREQUENCY = 31.1 kHz
MAY 10, 1971
·1744-1752
+1815-1821
E = cB
MAGNETIC RECEIVER
NOISE LEVEL
$\frac{B^2}{\Delta f}$, MAGNETIC FIELD SPECTRAL DENSITY
(GAMMA^2 Hz^{-1})
10^{-11}
10^{-12}
10^{-13}
10^{-14}
10^{-14}
10^{-13}
10^{-12}
10^{-11}
10^{-10}
10^{-9}
$\frac{E^2}{\Delta f}$, ELECTRIC FIELD SPECTRAL DENSITY
(VOLTS^2 METER^{-2} Hz^{-1})

Figure 15

Figure 16 The ratio E/cB calculated for the noise bands shown in Figure 15. The vertical bars indicate the precision of measurement of the value of the wave magnetic field resulting from the digitizing step size and subtraction of the magnetic receiver noise level spectral density. These ratios are somewhat smaller than the value of 1000 computed by Taylor [1973] for upper hybrid resonance noise inside the plasmasphere.

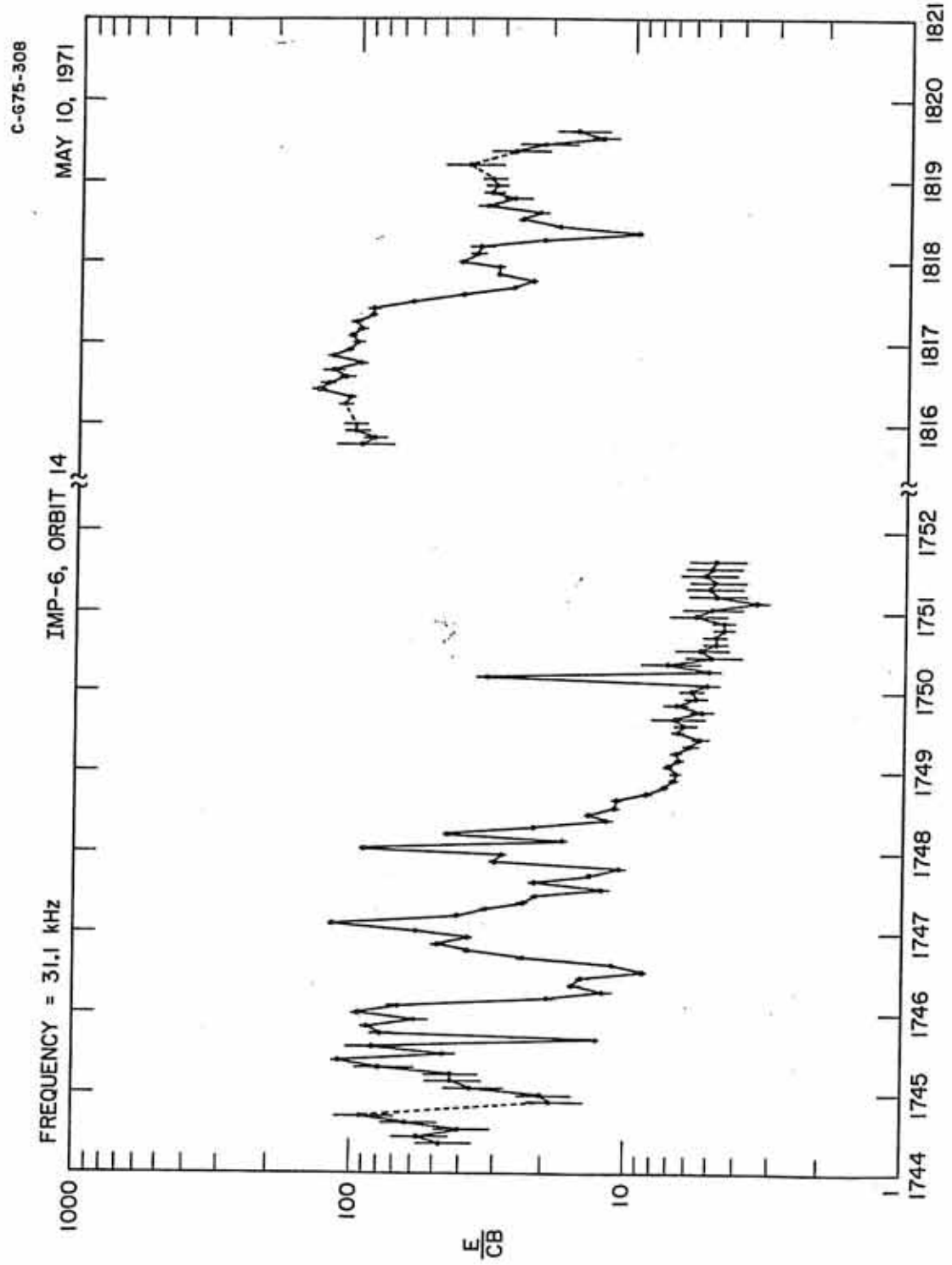
C-675-308
MAY 10, 1971
IMP-6, ORBIT 14
FREQUENCY = 31.1 kHz
E/CB
1000
100
10
1
1744
1745
1746
1747
1748
1749
1750
1751
1752
1816
1817
1818
1819
1820
1821
UT (HRS)

Figure 16

Figure 17 An example of diffuse electrostatic noise with a sharp upper cutoff frequency and a sharp lower cutoff frequency that exists for about twenty minutes. The electric field vector is oriented perpendicular to the geomagnetic field at the upper cutoff frequency and parallel to the geomagnetic field at the lower cutoff frequency. This type of noise has characteristics similar to the upper hybrid resonance noise observed at lower altitudes in the plasmasphere and ionosphere, but the frequency at which the noise occurs is strongly controlled by harmonics of the electron gyrofrequency when it is observed at radial distances outside the plasmasphere.

D-G72-447-4

IMP-6 UNIVERSITY OF IOWA PLASMA WAVE EXPERIMENT

ORBIT 48

SEPTEMBER 28, 1971

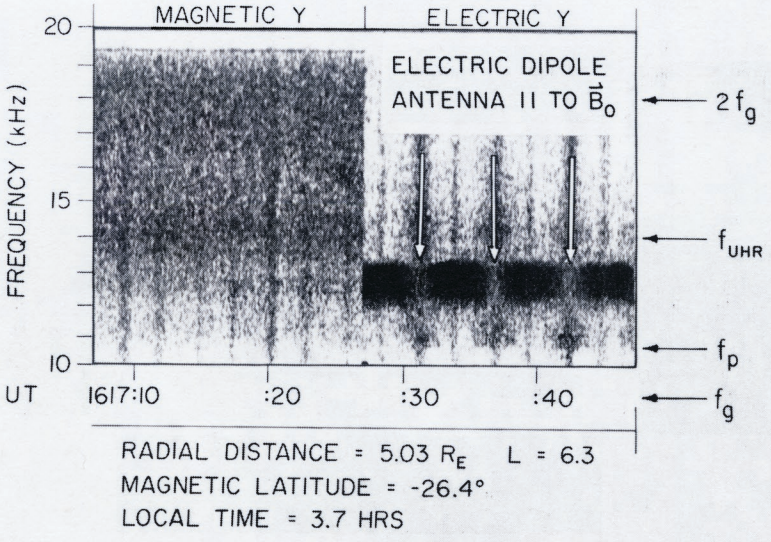

RADIAL DISTANCE = 5.03 R_E L = 6.3
MAGNETIC LATITUDE = -26.4°
LOCAL TIME = 3.7 HRS

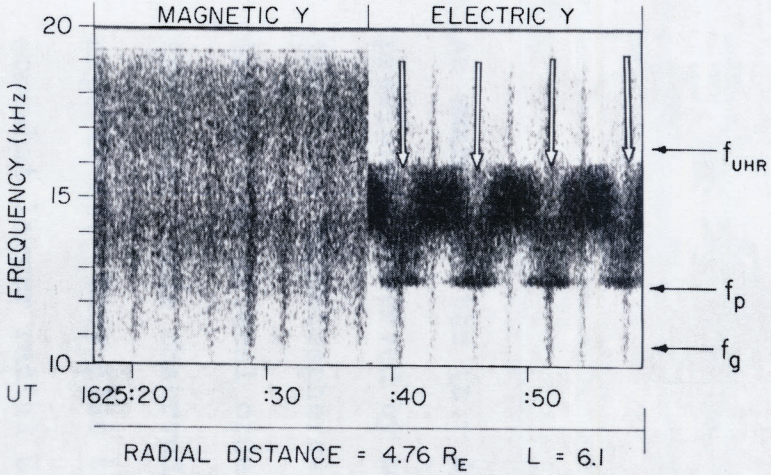

RADIAL DISTANCE = 4.76 R_E L = 6.1
MAGNETIC LATITUDE = -27.7°
LOCAL TIME = 3.9 HRS

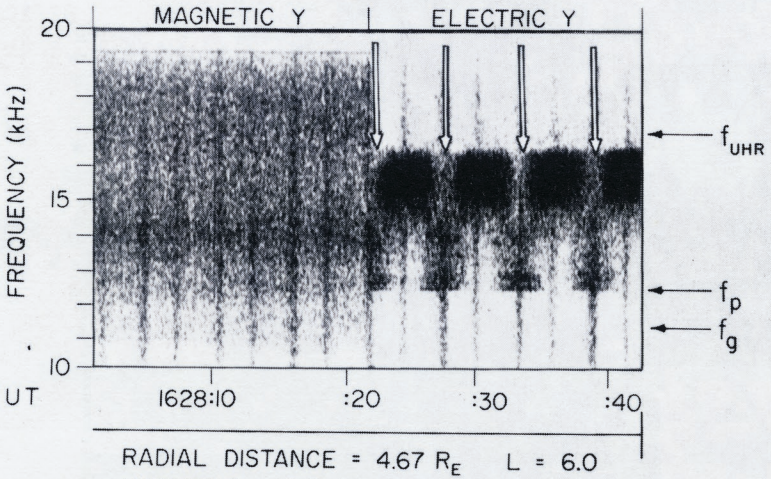

RADIAL DISTANCE = 4.67 R_E L = 6.0
MAGNETIC LATITUDE = -28.1°
LOCAL TIME = 4.0 HRS

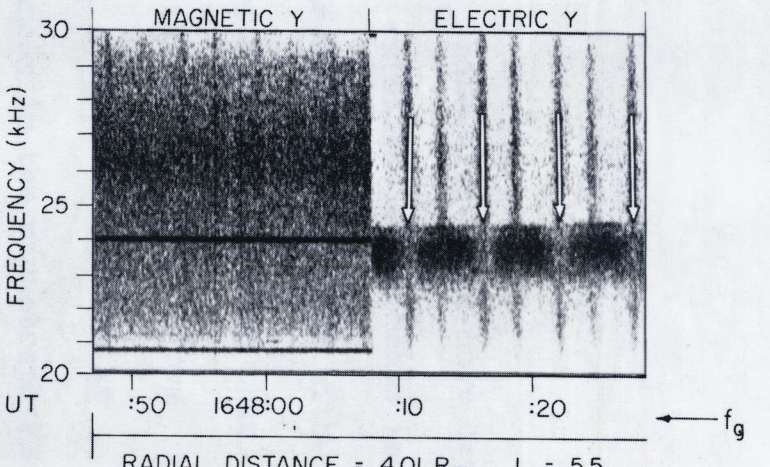

RADIAL DISTANCE = 4.01 R_E L = 5.5
MAGNETIC LATITUDE = -31.4°
LOCAL TIME = 4.5 HRS

Figure 18 An example of $(n + 1/2)f_g$ harmonics that have been previously observed by OGO 5 in the outer magnetosphere. These harmonics occur at somewhat larger radial distances in the magnetosphere and have different spectral characteristics than the electrostatic noise bands observed by the University of Iowa experiment. They also have broadband electric field strengths about three orders of magnitude larger than those typical of the diffuse and narrow band electrostatic noise. In many cases, however, the electrostatic noise bands have been observed to merge continuously into regions which contain $(n + 1/2)f_g$ harmonics.

A-G73-648

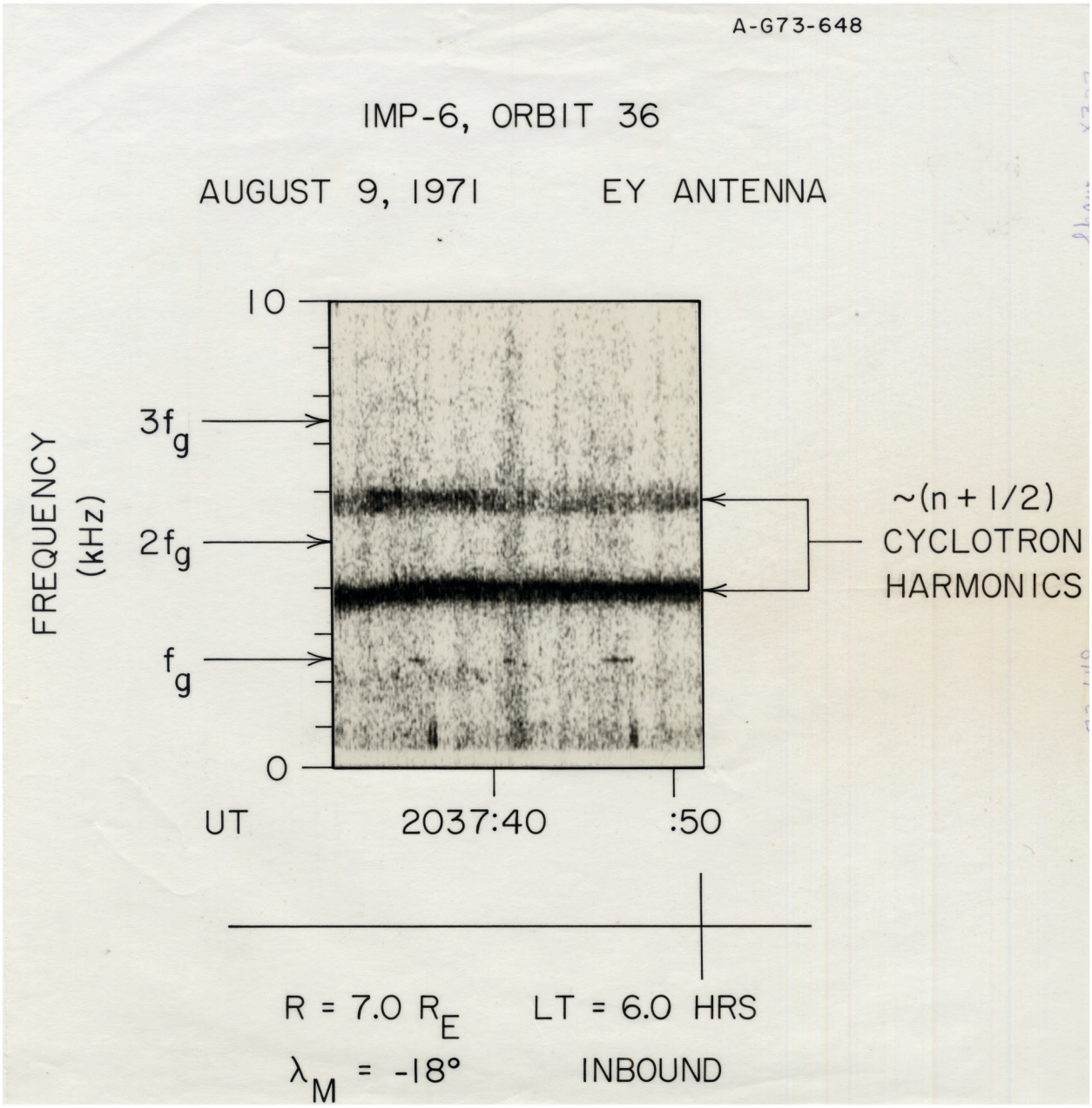
IMP-6, ORBIT 36
AUGUST 9, 1971
EY ANTENNA
10
3fg
2fg
fg
0
FREQUENCY (kHz)
~(n + 1/2) CYCLOTRON HARMONICS
UT
2037:40
:50
R = 7.0 RE
λM = -18°
LT = 6.0 HRS
INBOUND

Figure 19 An idealized representation of the dayside magnetosphere showing the types of noise discussed in this report. The local plasma frequency, upper hybrid resonance frequency, and electron gyrofrequency are shown as a function of geocentric radial distance. The continuous transition between the upper hybrid resonance noise inside the plasmasphere, the electrostatic noise bands observed by the University of Iowa experiment outside the plasmasphere, and the $(n + 1/2)f_g$ harmonics at larger radial distances in the outer magnetosphere is schematically illustrated.

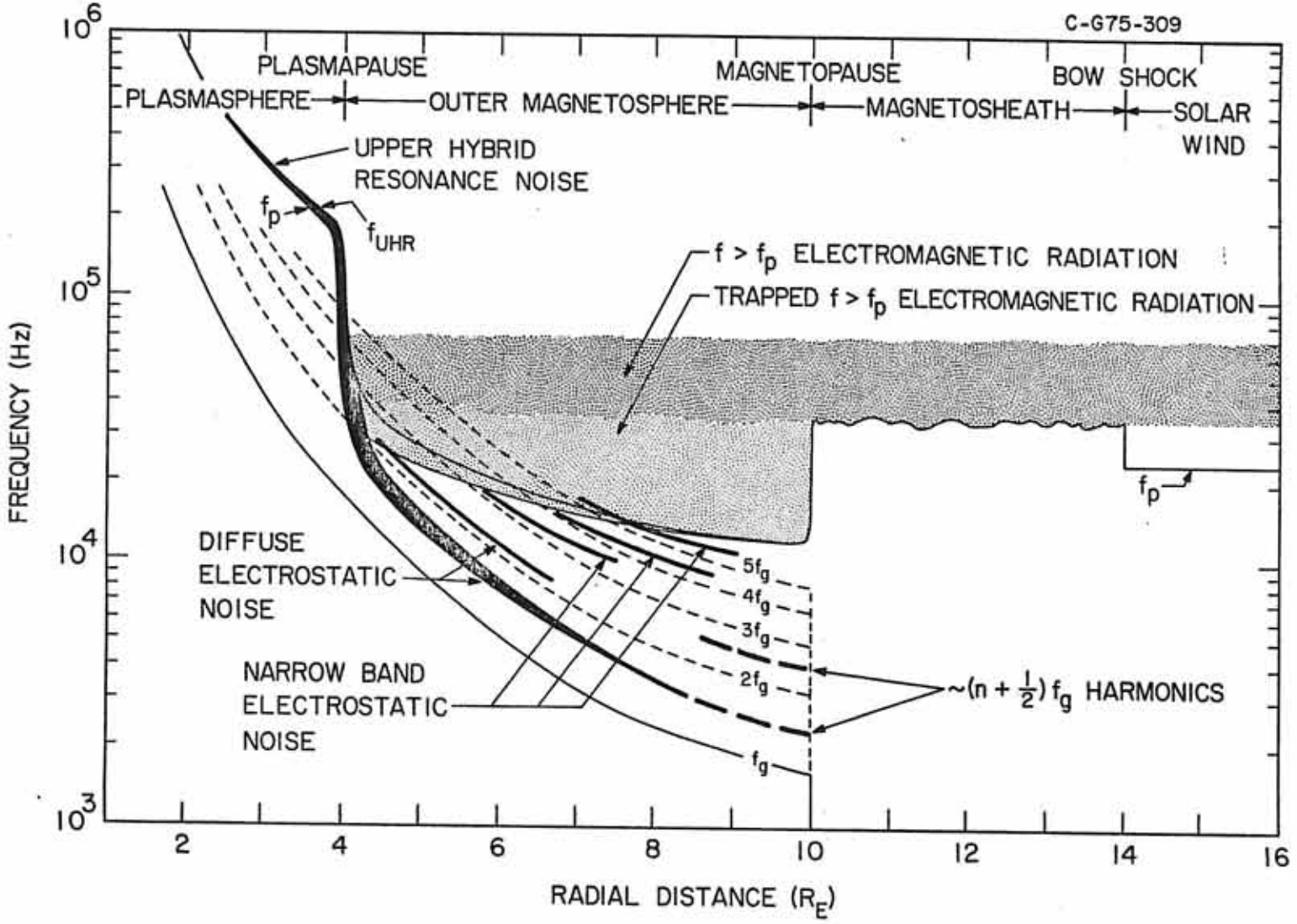
C-G75-309
PLASMAPAUSE
MAGNETOPAUSE
BOW SHOCK
PLASMASPHERE
OUTER MAGNETOSPHERE
MAGNETOSHEATH
SOLAR WIND
UPPER HYBRID RESONANCE NOISE
f_p
f_{UHR}
$f > f_p$ ELECTROMAGNETIC RADIATION
TRAPPED $f > f_p$ ELECTROMAGNETIC RADIATION
f_p
DIFFUSE ELECTROSTATIC NOISE
$5f_g$
$4f_g$
$3f_g$
$2f_g$
NARROW BAND ELECTROSTATIC NOISE
$\sim(n + \frac{1}{2}) f_g$ HARMONICS
f_g
FREQUENCY (Hz)
10^6
10^5
10^4
10^3
2
4
6
8
10
12
14
16
RADIAL DISTANCE (R_E)

Figure 19